A Szilikátipari Tudományos Egyesület lapja

építőanyag

Journal of Silicate Based and Composite Materials

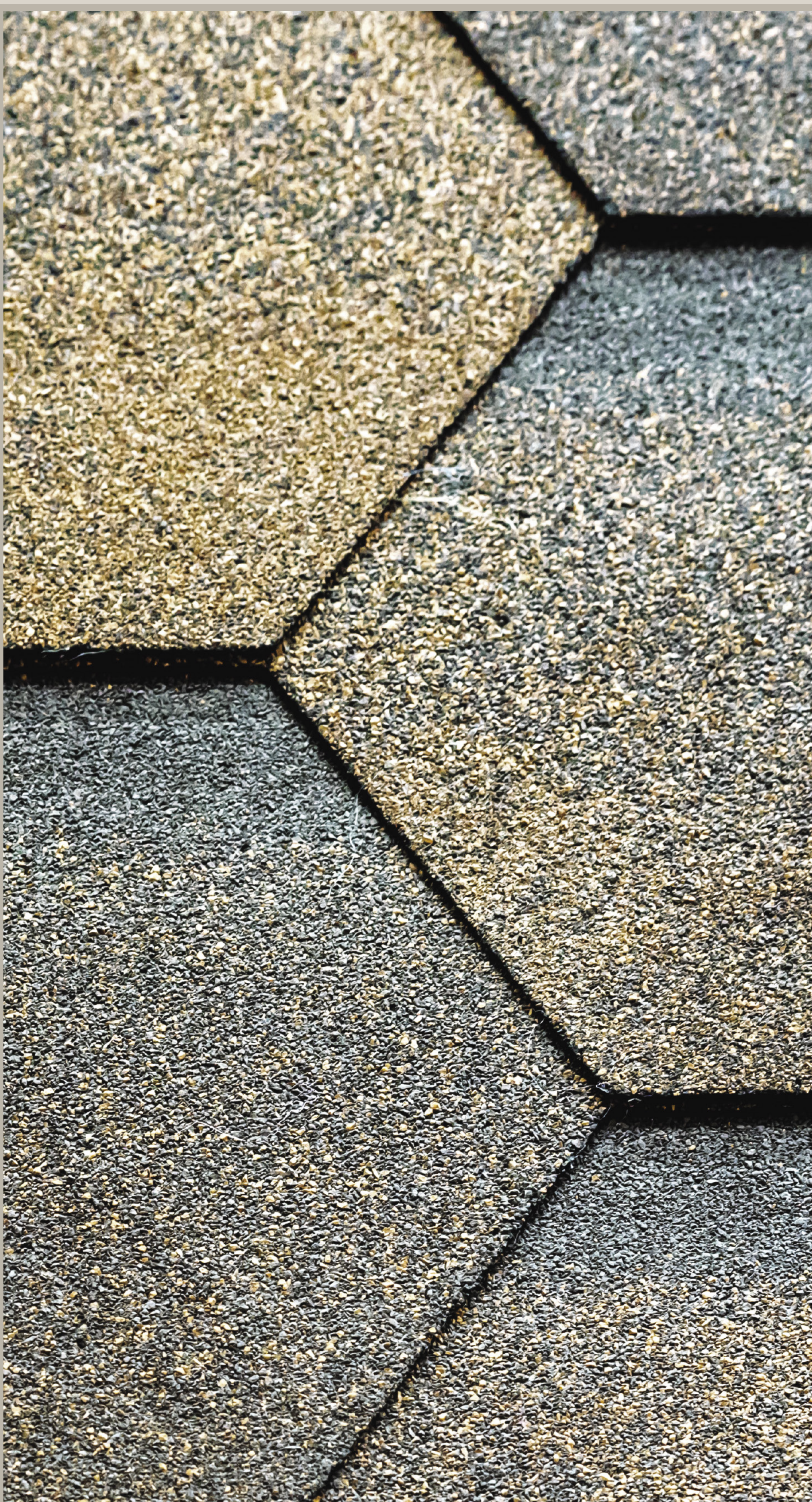

A TARTALOMBÓL:

2022/2

ECCM20

COMPOSITES MEET SUSTAINABILITY

26-30 JUNE 2022-LAUSANNE-SWITZERLAND

20TH EUROPEAN CONFERENCE ON COMPOSITE MATERIALS

Organized by

EPFL

Under the patronage of

ESCM
EUROPEAN SOCIETY FOR COMPOSITE MATERIALS

Conference Chair
Anastasios P. Vassilopoulos

Conference Co-Chair
Véronique Michaud

GENERAL INFORMATION

Four years after the previous even, the European Conference on Composite Materials celebrates its 20th edition in June 2022 organized by the Ecole Polytechnique Fédérale de Lausanne.

The ECCM brings together participants from academia and industry with common interests in all fields of Composite Materials. This dynamic conference is the European forum for knowledge exchange on the recent accomplishments and the future trends in Composite Materials. ECCM is the regular meeting point for composite specialists and newcomers and is traditionally the place where people meet each other and establish long lasting friendships and collaborations.

The Conference Theme is **"Composites meet Sustainability"**

ECCM20 includes plenary talks, keynote lectures, oral and poster presentations, and an entertaining social program for delegates from around the world. The event layout and schedule will provide many opportunities to network, learn, discuss and share with colleagues from across the world.

ECCM20 is organized for the first time in Switzerland, at the magnificent region of the Swiss Riviera, promising an unforgettable experience.

We are looking forward to welcoming you in Lausanne in 2022

KEY DATES

01 June 2021
Registration open/first announcement

15 November 2021
Abstract submission deadline

1 February 2022
Author notification for acceptance

16 March 2022
Full paper submission

1 April 2022
Early bird registration

26-30 June 2022
ECCM20 @ EPFL

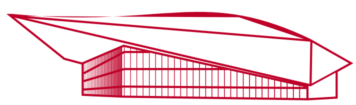

LOCATION

The ECCM20 will be hosted by EPFL at the Swiss Tech Convention Center (www.stcc.ch). The SwissTech Convention Center is one of the largest conference centers in the Lake Geneva region, hosting events of international fame. This majestic building is distinguished by its modernity, its innovative technologies and a warm and experienced team.

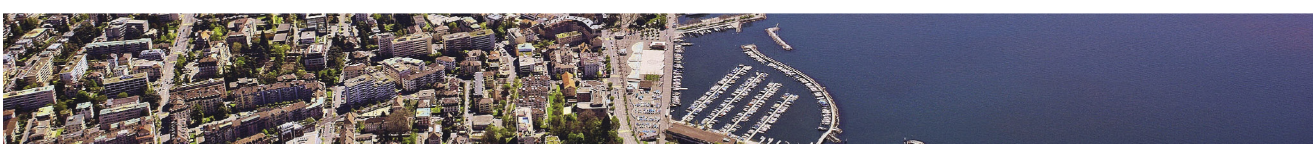

WWW.ECCM20.ORG

építőanyag

Journal of Silicate Based and Composite Materials

2022/2

TARTALOM

CONTENT

A finomkerámia-, üveg-, cement-, mész-, beton-, tégla- és cserép-, kő- és kavics-, tűzállóanyag-, szigetelőanyag-iparágak szakmai lapja
Scientific journal of ceramics, glass, cement, concrete, clay products, stone and gravel, insulating and fireproof materials and composites

A folyóiratot referálja · The journal is referred by:

A folyóiratban lektorált cikkek jelennek meg.
All published papers are peer-reviewed.
Kiadó · Publisher: Szilikátipari Tudományos Egyesület (SZTE)
Elnök · President: ASZTALOS István
1034 Budapest, Bécsi út 120.
Tel.: +36-1/201-9360 ▪ E-mail: epitoanyag@szte.org.hu
Tördelő szerkesztő · Layout editor: NÉMETH Hajnalka
Címlapfotó · Cover photo: GYURKÓ Zoltán

WWW.EPITOANYAG.ORG.HU
EN.EPITOANYAG.ORG.HU

Online ISSN: 2064-4477
Print ISSN: 0013-970x
INDEX: 2 52 50 ▪ 74 (2022) 43–77

Observation of shear bond strength between zirconia core and silica based composite material; a finite element analysis

Koray SOYGUN ▪ Faculty of Dentistry, Cukurova University, Turkey ▪ koraysoygun@hotmail.com
Zafer ÖZER ▪ Mersin Vocational High School Electronic and Automation Department, Mersin University, Turkey ▪ zaferozer@hotmail.com
Cem KURTOGLU ▪ Faculty of Dentistry, Cukurova University, Turkey ▪ ckurtoglu33@gmail.com
Amirullah M. MAMEDOV ▪ Nanotechnology Research Center (NANOTAM), Bilkent University, Turkey ▪ mamedov46@gmail.com
Ekmel OZBAY ▪ Department of Physics, Bilkent University, Turkey ▪ ozbay@bilkent.edu.tr

Érkezett: 2021. 05. 21. ▪ Received: 21. 05. 2021. ▪ https://doi.org/10.14382/epitoanyag-jsbcm.2022.7

Abstract

The strength of all-ceramic restorations depends on not only properties of basic material but also used ceramic material, substructure and upper structure connection, the thickness of crown, design, and bonding technique of restoration. The purpose of this study is to analyze the shear stress between the zirconia core and silica-based ceramic by using the finite element method. Using 20-node structural solid elements, the shear stresses were calculated with the methods of shear test and Schmitz-Schulmeyer test through 3-dimensional finite element method. The commercial software Ansys (Ansys Version 11.0, ANSYS, Inc., Canonsburg, PA 15317, USA) was used to create a three-dimensional mesh. There is no significant difference between the test methods as a result of the force applied close to the bond interface. However, when moving away from the bond interface, it is understood that there is a failure in higher tensile forces. It was determined that there was no significant difference in the results when the force to be applied in both the Shear bond Test and Schmitz-Schulmeyer tests was performed the near interface of Zirconia core-Silica based veneer ceramic.

Keywords: silica based composite; finite elements analysis; shear strength; Schmitz-Schulmeyer; zirconia

Kulcsszavak: szilícium-dioxid alapú kompozit; végeselemes analízis; nyírószilárdság; Schmitz-Schulmeyer; cirkónia

Koray SOYGUN
Prof. of Department of Prosthodontics, Faculty of Dentistry, Cukurova University. Conducts research on many Composite Dental materials.

Zafer ÖZER
Assoc. Prof. of Department of Automation and Electronics, Mersin Vocational High School, Mersin University. Conducts research on materials, photonics crystals and phononic crystals.

Cem KURTOGLU
Prof. Dr., Head of Department of Prosthodontics, Faculty of Dentistry, Cukurova University. Conducts research on many Dental materials.

Amirullah M. MAMEDOV
Prof. of NANOTAM, Nanotechnology Research Center, Bilkent University. Conducts research on physico-mechanical properties of materials and metamaterials.

Ekmel OZBAY
Prof. of NANOTAM, Nanotechnology Research Center, Bilkent University. Conducts research on materials and metamaterials.

1. Introduction

Recent developments in dentistry for materials and technology have increased the aesthetic expectations. Ensuring the shade harmony between the specified shade and the natural shade of teeth is one of the most important criteria of success in the aesthetic sense. Nowadays, many ceramic materials and systems are used, and the clinical activities of these systems have been discussed in many scientific articles, and the differences between each other have been investigated [1]. Although metal-reinforced restorations are widely used, they can remain aesthetically inadequate due to their metal cores [2]. Despite the success of metal-ceramic restorations on power and impact endurance, researchers have not stopped looking for new materials [3]. All-ceramic restorations have gained great popularity in the last 10 years [4]. All-ceramic restorations are more aesthetic than metal-ceramic restorations, and this is one of the most important factors in the increase of their use [5]. In other words, all-ceramic restorations are more aesthetically superior because they have different optical properties than metal-reinforced ceramic restorations. Today, there are a large number of materials that are fully ceramic-based such as leucite-reinforced ceramics, glass-infiltrated ceramics, lithium disilicate, alumina, and zirconia [6]. In these, zirconia offers better mechanical properties. High durability, white appearance, chemical, and structural stability are the features that bring the zirconia core to the forefront. [7].

To obtain the optimum aesthetics, the zirconia cores are covered with silica based ceramic materials. Then, by adding veneer ceramics to the layer, certain restorations are provided according to the individual's optical characteristics. Zirconium substructure is resistant to damage from abrasions caused by sharp corners and internal adaptations sourced from the structure of teeth and durable to the pressures of chewing. Zirconia has a high bending resistance due to its transformation hardness characteristic, which puts itself ahead of other materials. It is biocompatible, which is also an important good feature. Covering the Zirconia core with silica based ceramic is better for its aesthetic appearance, while the weakness of fracture strengths is one of the disadvantages of zirconia-based restorations [7,8].

Different tests can be found in the literature on the determination of the shear stresses of Veneer ceramics [9]. Ozkurt et al. have applied Shear tests using the ceramics of 4 different manufacturers [10]. They also conducted a surface crack analysis to determine the errors. They found the highest shear voltage value as 40.49±8.43 MPa in the products of DC-Zirkon Company. In their study, they determined that shear stresses differ according to the type of zirconia used by the manufacturer.

Tuncel et al. investigated the effects of shading in zirconia veneering on shear stresses [11]. In the study, zirconia discs were divided into 11 groups, each of which were 12 pieces, and they used shear test method when examining the shading stress. As a result of their work, they found the lowest shear stress as 29.47 MPa and the highest shear stress as 36.40 MPa. As a result of their experiments, they determined that shadingprocesses affect the zirconia/ceramic shear stress, and the results they find showed that the study is clinically acceptable.

Teng et al. used the Schmitz-Schulmeyer test method to detect shear stresses in all-ceramic systems [12]. In the study, they used 30 zirconia core ceramics coated with veneering ceramics. They used three different surface leveling methods: surface leveling with silicon carbide disc, aluminum particles, airborne-particle abrasion and powder-coated zirconia. They used a metal-ceramic system as a control group and investigated their differences with all-ceramics in the results section. The average shear stresses of the control group were investigated with three different surface levels and was 47.02 MPa for powder-coated zirconia, 39.14 MPa for particle abrasion, 36.66 MPa for silicon carbide disc, and 46.12 MPa for the control group.

Guess et al. investigated the differences of the shear stresses between the core and veneering ceramics in all-ceramics belonging to different companies and their sensitivities to heat exchange through the Schmitz-Schulmeyer test method [13]. This study used a metal-ceramic system as a control group. The temperature range for which sensitivity is measured is 5-55 °C. They observed different shear stress values for different brands. Consequently, the shear stresses between the core ceramics and silica based ceramics are not affected by heat exchange [13].

The finite element method (FEM) is a numerical technique used by different disciplines in the field of engineering [14]. It provides cost and time savings during the modeling phase of the processes. Modeling of many materials can be done with FEM. In the application of dentistry, FEM is used in the analysis of the success of the all-ceramic restorations [15]. The calculation of shear stresses between core ceramics and veneer ceramics and the multifaceted examination can be done with FEM [16]. In this study, shear stresses between core ceramic and silica based ceramic in all-ceramic restorations were tested using shear Test and Schmitz-Schulmeyer test methods. The application was performed using FEM.

2. Materials and methods

In the present study, FEM was used for all calculations to detect shear stresses in all-ceramic restorations. Using 20-node structural solid elements, the shear stresses were calculated with the methods of shear test and Schmitz-Schulmeyer test through 3-dimensional FEM.

The commercial software Ansys (Ansys Version 11.0, ANSYS, Inc., Canonsburg, PA 15317, USA) was used to create a three-dimensional mesh which the model 1 (3D model used for shear testing, *Fig. 1*) consisting 9060 nodes with 42789 mainly tetrahedral elements and the model 2 (3D model used for Schmitz-Schulmeyer test, *Fig. 2*) consist of 12858 nodes with 8339 mainly tetrahedral elements.

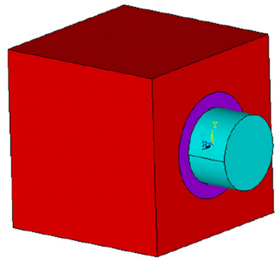

Fig. 1 *3D model used for shear testing*
1. ábra *A nyírószilárság teszteléséhez használt 3D modell*

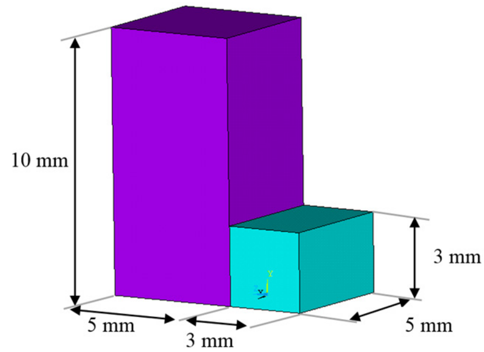

Fig. 2 *3D model used for Schmitz-Schulmeyer test*
2. ábra *A Schmitz-Schulmeyer vizsgálathoz használt 3D modell*

The Solid 92 element was divided into meshes with a 10-node tetrahedral element, which yields results closer to reality than the 4-node tetrahedral element, but with a longer solution duration.

This element has three degrees of displacement (u_x, u_y, u_z) at each node x, y, z direction, and is suitable for the solution of large displacements, large strain, slip and plasticity problems (*Fig. 3*).

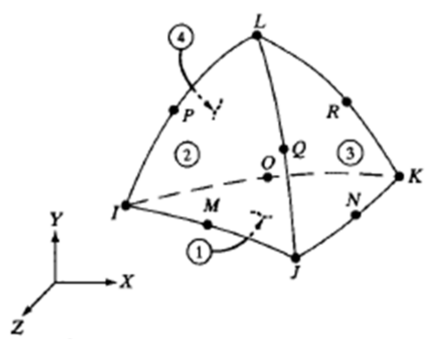

Fig. 3 *10 node Solid 92 element*
3. ábra *10 csomópontú Solid 92 elnevezésű végeselem*

The mechanical properties of the materials used in the analysis are given (*Table 1*).

Materials	Young's Modulus (MPa)	Poisson Ratio
Acrylic resin	33×10^2	0.30
Zirconia Core Ceramic	1×10^5	0.25
Silica based Veneer Ceramic	65×10^3	0.19

Table 1 *The mechanical properties of the materials used in the analysis*
1. táblázat *A felhasznált anyagok mechanikai tulajdonságai*

2.1 Shear test

In the 3D analysis, a cylinder with a core ceramic structure with a radius of 3.5 mm was placed inside a cube made of 12 mm acrylic material for shear testing (*Fig. 1*). The silica based veneer ceramic material in cylindrical structure with radius of 2.5 mm is bonded to the core ceramic material. The cylinder height is 3 mm. Acrylic and core ceramics were divided into meshes with 3-dimensional tetra hedra elements. To apply the force to the desired location, the silica based veneer ceramic material was divided into meshes with hexahedra elements. The force was applied to 3 different regions as shown (*Fig. 4*) and the applied force is 200 N. The application area of the force is in the form of sharp knives (*Fig. 3*) but is a wider range of enforcement areas (*Fig. 3-b*).

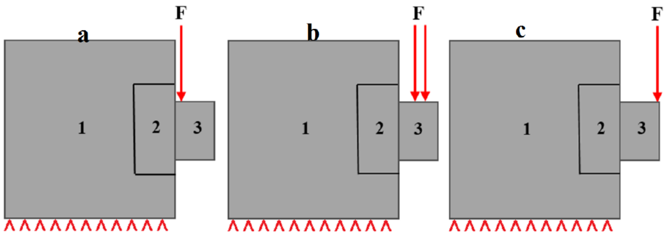

Fig. 4 (1) Acrylic resin, (2) Zirconia Core Ceramic, (3) Silica based Veneer Ceramic, (a) Force applied to the region near the interface of Zirconia core-silica based veneer ceramic, (b) Force applied to the large surface area of silica based veneer ceramic, (c) Force applied to the end of the silica based veneer ceramic

4. ábra (1) akrilgyanta, (2) cirkónium-oxid kerámia, (3) szilícium-dioxid alapú furnérkerámia, (a) a cirkónium szilícium-dioxid alapú furnérkerámia határfelületéhez közeli területre kifejtett erő, (b) a szilícium-dioxid alapú furnérkerámia felületére kifejtett erő, (c) A szilícium-dioxid alapú furnérkerámia szélére alkalmazott erő

As the boundary condition for this model, the nodes at the bottom of the acrylic resin were fixed as shown (*Fig. 3a*). It is assumed that all three materials are linear, elastic and isotropic.

2.2 Schmitz-Schulmeyer test

For Schmitz-Schulmeyer test, two rectangular prisms glued together were designed in 3D analysis as shown (*Fig. 2*). The core ceramic material was modeled with a rectangular prism of 5x5x10 mm and silica based veneer ceramic material with a rectangular prism of 3x5x3 mm. The force was applied in three different ways, as shown (*Fig. 5 a-c*), and the applied force is 200 N.

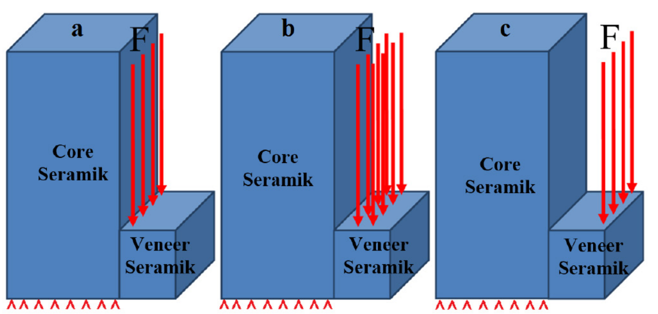

Fig. 5 (a) Force applied to the region near the interface of Zirconia core- silica based veneer ceramic, (b) Force applied to the large surface area of silica based veneer ceramic, (c) Force applied to the end of the silica based veneer ceramic

5. ábra (a) A cirkónium szilícium-dioxid alapú furnérkerámia határfelületéhez közeli területre kifejtett erő, (b) A szilícium-dioxid alapú furnérkerámia felületére kifejtett erő, (c) A szilícium-dioxid alapú furnérkerámia végére kifejtett erő

As a boundary condition for this model, the nodes at the bottom of the core ceramic material were fixed. It was assumed that the two materials are linear elastic and isotropic.

3. Results and discussion

In all-ceramic restorations, the shear bond test (*Fig. 4*) and Schmitz-Schulmeyer test (*Fig. 5*) were modeled and analyzed with finite element method to detect shear stresses between core ceramics and silica based veneer ceramics. The maximum shear stresses obtained from the analyses were given (*Table 2*).

For shear bond test, the results of shear stresses obtained as a result of forces applied to positions (Figs. 4,6).For Schmitz-Schulmeyer test, the results of shear stresses obtained as a result of forces applied to positions (*Figs. 5,7*).

	Shear Test (MPa)	Schmitz-Schulmeyer Test (MPa)
Near interface of Zirconia core-Silica based veneer ceramic	63.05	64.45
Wide surface of silica based veneer ceramics	47.04	100.58
Endpoint of silica based veneer ceramic	265.26	369.43

Table 2 The maximum shear stresses obtained from the analyses (MPa)

2. táblázat A számításokból meghatározott maximális nyírófeszültség (MPa)

The more aesthetic demands expected from dental restorations have increased the clinical use of all-ceramic restorations. With the development of zirconium oxide-based core materials, strong core and aesthetic veneer ceramic combinations have been successfully used. In order for zirconium oxide-based restorations to provide long-term functional, biological, and aesthetic requirements, the bond between reinforced core and esthetic veneer ceramic must be successful [17]. Luthardt et al. [18] indicated that failure in zirconium oxide systems mostly occurred on two porcelain interfaces.

The presence of zirconium oxide monoclinic phase on the interface of zirconium oxide-based restorations with core and veneer porcelain may result in the formation of intermediate micro-spaces[19]. Phase transformation occurring in zirconium oxide can trigger the formation of localized stresses that cause micro cracks in the veneer porcelain. The thermal expansion coefficient of the monoclonal phase in zirconium oxide ceramics is 7.5 x 106 K^{-1}, and the thermal expansion coefficient of the tetragonal phase is 10.8 x 106 K^{-1}[19]. For these reasons, it is reported that t → m transformation occurring on the surface of zirconium oxide ceramics can affect the bond strength between the core and silica based veneer porcelain [20].

Limited in vivo studies that evaluate zirconium oxide-reinforced core restorations indicate that the most common failure in such restorations is that whole or part of the veneer porcelain can separate from the core in the form of layers [21]. It is thought that many factors are involved in the occurrence of this problem. These can be sorted as a lack of proper geometry of the core, fatigue phenomenon, in-ceramic defects, insufficient core support, lack of occlusal stability, patient-dependent factors, inadequate bonding force, discrepancy between the core, and the thermal expansion coefficients of the materials used in the core and veneer [7,22]. Although the factors affecting the bond in the interface are known, but the bond between the core and the veneer has still been not clearly explained.

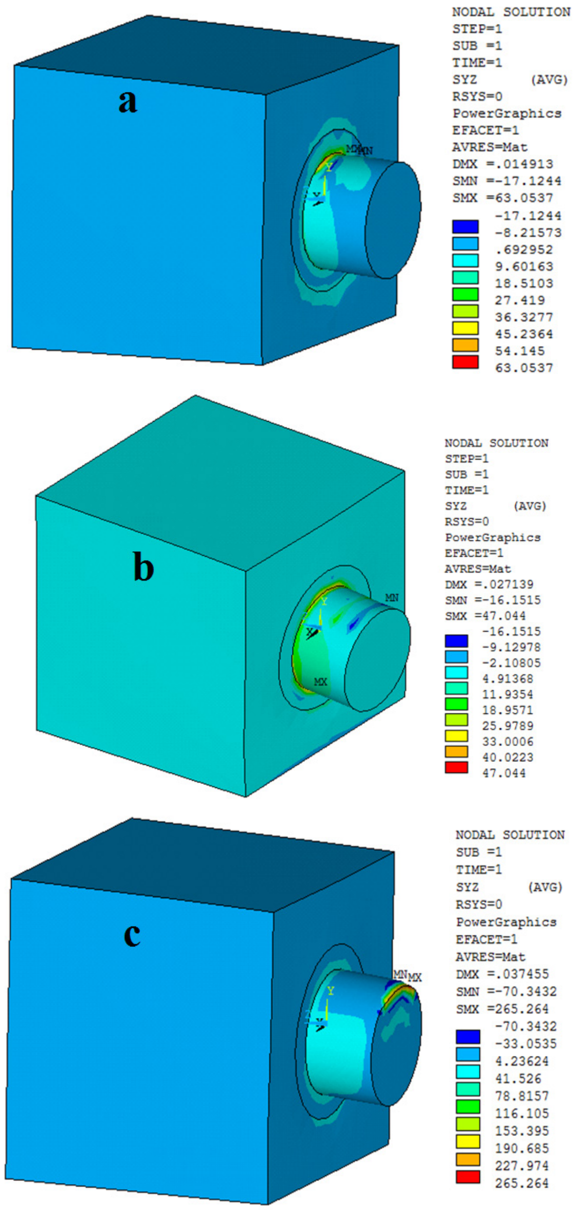

Fig. 6 According to the force applied to areas, shear stress results (a) near the interface of Zirconia core-silica based veneer ceramic, (b) the large surface area of silica based veneer ceramic, (c) the end of the silica based veneer ceramic

6. ábra Az alkalmazott terhelésekből számolt nyírófeszültség (a) a cirkónium-dioxid alapú furnérkerámia határfelülete közelében, (b) a szilícium-dioxid alapú furnérkerámia felületén, (c) a szilícium-dioxid alapú furnérkerámia szélén

In a study, which evaluated the fixed-section prostheses with 3 to 5-member zirconium oxide core in the posterior region on 45 patients during 3 years of use, the failure of the veneering to separate from the core was revealed as 13% [21]. In a prospective clinical pilot study that investigated the activities of the three-member zirconium oxide core prostheses in the posterior region, the 20 three-member zirconium oxide core prostheses with fixed-section were followed up on 16 patients during 3 years, consequently the minor fractures were observed in the veneer porcelain in the five of the fixed-section prostheses [23]. At the end of the 2-year follow-up period of 20 zirconium oxide core with 3-5 members fixed part prosthesis by using DC zirconium technique, they reported that fractures in the veneer porcelains were observed in 15% of the restorations[24].

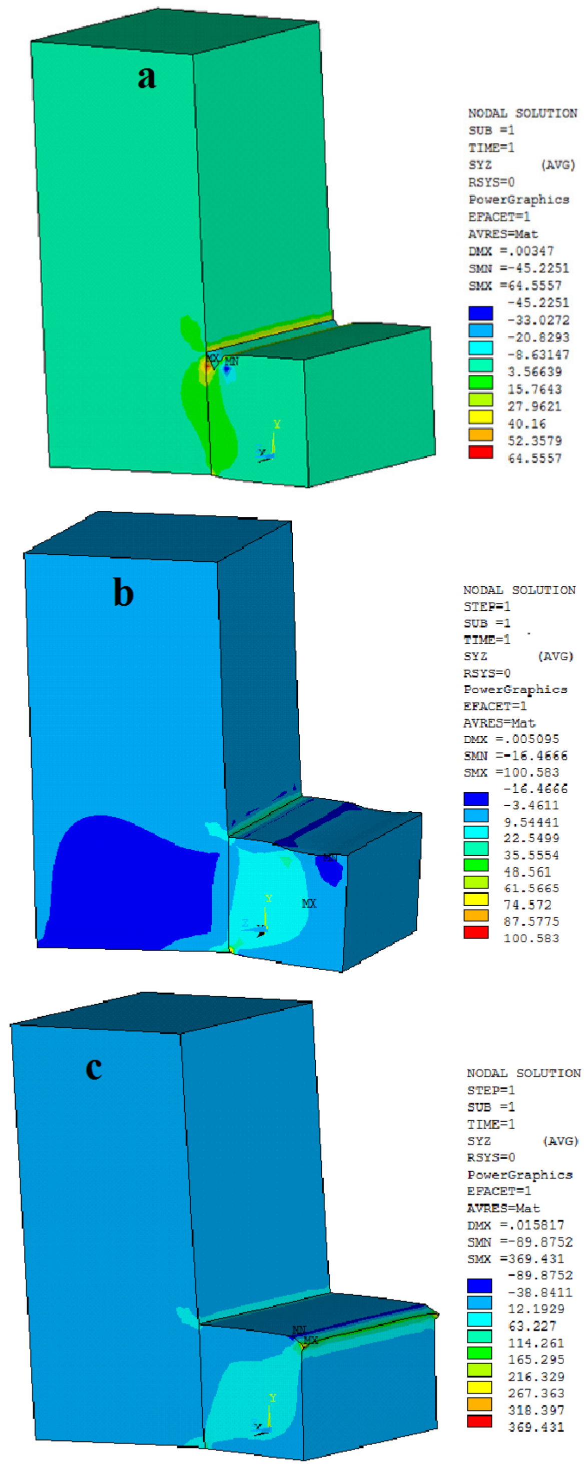

Fig. 7 According to the force applied to areas in Schmitz-Schulmeyer test, shear stress results (a) near the interface of Zirconia core-silica based veneer ceramic,(b) the large surface area of silica based veneer ceramic, (c) the end of the silica based veneer ceramic

7. ábra A Schmitz-Schulmeyer teszt során a kifejtett erő szerint a nyírófeszültség értéke (a) a cirkónium-oxid szilícium-dioxid alapú furnérkerámia határfelülete közelében, (b) a szilícium-dioxid alapú furnérkerámia felületén, (c) a szilika alapú furnérkerámia szélén

In the present study, we compared the bond strength between zirconia core and silica based porcelain by using shear bond test and Schmitz-Schulmeyer test methods with finite element analysis in both test methods and obtained a stress of 64.45 MPa with shear test and 63.05 MPa with Schmitz-Schulmeyer test for near interface of zirconia core-veneer ceramic. With the force applied to the wide surface of veneer ceramics, 47.04 and 100.58 MPa stress were obtained, respectively. In addition, with the force applied to the veneer ceramic endpoint, which is the third force application point, the stress was 265.26 MPa with shear test and 369.43 MPa with Schmitz-Schulmeyer test. *Table 2* shows that there is no significant difference between the test methods as a result of the force applied close to the bond interface. However, when moving away from the bond interface, it is understood that there is a failure in higher tensile forces. At the same time, bond strength assessment with Schmitz-Schulmeyer test application may result in failure due to higher forces.

A study, where the bond strength is tested on different core and porcelain surfaces by the Schmitz-Schulmeyer test method, reported that bone strength in zirconia core and silica based porcelain interfaces was not better than metal ceramics, and this bone strength was not affected by thermal cycles [13].

In the literature, there are studies that compare the bond strength values between different core materials and dental ceramics [4,9,10,11,13]. In the present study, both the test methods and the bond failure at different distances of the applied force to the bond interface were evaluated by finite element analysis. If the distance to the bone interface increases, we can say that the bone strength occurs as a result of applying force at higher values. We can also propose that the higher bone strength values with the Schmitz-Schulmeyer test application are due to the larger bond surface area.

One of the factors that affect the success of the treatment with complete ceramic systems is the choice of the right material. Two experimental methods used in dentistry to measure shear stresses in all-ceramic restorations are Shear bond Test and Schmitz-Schulmeyer test. In experimental tests, there is not much data available, and there is also a time and cost problem. With finite element analysis, both methods can be done using more materials at a lower cost and in less time. In addition, it is possible to analyze shear stresses in all-ceramic systems in a versatile way by finite element analysis.

4. Conclusions

As a result of our finite element analysis study, in vitro experimental studies investigating the shear bond strength of zirconia and feldspathic ceramic materials of all-ceramic restorations, it was determined that there was no significant difference in the results when the force to be applied in both the shear bond test and Schmitz-Schulmeyer tests was performed the near interface of zirconia core-Silica based veneer ceramic. However, it has been observed that the difference in test methods significantly affects the results in the case of applying a load from the wide surface or the endpoint of silica based veneer ceramic of the connection.

References

[1] Conrad HJ, Seong WJ, Pesun IJ (2007) Current ceramic materials and systems with clinical recommendations: a systematic review. Journal of Prosthetic Dentistry, Vol. 98, pp. 389-404, https://doi.org/10.1016/S0022-3913(07)60124-3

[2] Raigrodski AJ (2004) Contemporary materials and technologies for all-ceramic fixed partial dentures: a review of the literature. Journal of Prosthetic Dentistry, Vol. 92, pp. 557-562, https://doi.org/10.1016/j.prosdent.2004.09.015

[3] Fischer H, Marx R (2002) Fracture toughness of dental ceramics: comparison of bending and indentation method. Dental Materials, Vol. 18, pp. 12-19, https://doi.org/10.1016/S0109-5641(01)00005-7

[4] Aboushelib MN, De Jager N, Kleverlaan CJ, Feilzer AJ (2005) Microtensile bond strength of different components of core veneered all-ceramic restorations. Dental Materials, Vol. 21, pp. 984-991, https://doi.org/10.1016/j.dental.2005.03.013

[5] Wall JG, Cipra DL (1992) Alternative crown systems. Is the metal-ceramic crown always the restoration of choice?. Dental Clinic of North America, Vol. 36, pp. 765-782.

[6] Soygun K, Varol O, Ozer A, Bolayir G (2017) Investigations on the effects of mouthrinses on the colour stability and surface roughness of different dental bioceramics. Journal of Advanced Prosthodontics, Vol. 9, pp. 200-207, https://doi.org/10.4047/jap.2017.9.3.200

[7] White SN, Miklus VG, McLaren EA, Lang LA, Caputo AA (2005) Flexural strength of a layered zirconia and porcelain dental all-ceramic system. Journal of Prosthetics Dentistry, Vol. 94, pp. 125–131, https://doi.org/10.1016/j.prosdent.2005.05.007

[8] Denry I, Kelly JR (2008) State of the art of zirconia for dental applications. Dental Materials, Vol. 24(3), pp. 299–307, https://doi.org/10.1016/j.dental.2007.05.007

[9] Mosharraf R, Rismanchian M, Savabi O, Ashtiani AH (2011) Influence of surface modification techniques on shear bond strength between different zirconia cores and veneering ceramics. Journal of Advanced Prosthodontics, Vol. 3, pp. 221-228, https://doi.org/10.4047/jap.2011.3.4.221

[10] Ozkurt Z, Kazazoglu E, Ünal A (2010) In vitro evaluation of shear bond strength of veneering ceramics to zirconia. Dental Materials Journal, Vol. 29, pp. 138-146, https://doi.org/10.4012/dmj.2009-065

[11] Tuncel I, Ozat P, Eroğlu E (2014) Effects of coloring procedures on zirconia/veneer ceramics bond strength. Journal of Advanced Prosthodontics, Vol. 6, pp. 451-455, https://doi.org/10.4047/jap.2014.6.6.451

[12] Teng J, Wang H, Liao Y, Liang X (2012) Evaluation of a conditioning method to improve core-veneer bond strength of zirconia restorations Journal of Prosthetic Dentistry, Vol. 107, pp. 380-387, https://doi.org/10.1016/S0022-3913(12)60095-X

[13] Guess PC, Kuliš A, Witkowski S, Wolkewitz M, Zhang Y, Strub JR (2008) Shear bond strengths between different zirconia cores and veneering ceramics and their susceptibility to thermocycling. Dental Materials, Vol. 24, pp. 1556-1567. https://doi.org/10.1016/j.dental.2008.03.028

[14] Brenner SC, Carstensen C (2004) Finite Element Methods. In: Stein E, de Borst R, Hughes TJR (eds) Encyclopedia of computational mechanics, Wiley, Weinheim, pp. 73-118.

[15] Fischer H, Weber M, Marx R (2003) Lifetime prediction of all-ceramic bridges by computational methods, Journal of Dental Research, Vol. 82, pp. 238-242, https://doi.org/10.1177/154405910308200317

[16] Motta AB, Pereira LC, Duda FP, Anusavice KJ (2014) Influence of substructure design and occlusal reduction on the stress distribution in metal ceramic complete crowns: 3D finite element analysis. Journal of Prosthodontics, Vol. 23, pp. 381-389, https://doi.org/10.1111/jopr.12119

[17] Fleming GJP, El-Lakwah SFA, Harris JJ, Marquis PM (2004) The Influence of interfacial surface roughness on bilayered ceramic specimen performance. Dental Materials, Vol. 20, pp. 142-149. https://doi.org/10.1016/S0109-5641(03)00085-X

[18] Luthardt RG, Sandkuhl O, Reitz B (1999) Zirconia-tzp and alumina-advanced technologies for the manufacturing of single crowns. European Journal of Prosthodontics and Restorative Dentistry, Vol. 7, pp. 113-119.

[19] Guazzato M, Pross K, Quach L, Swain MV (2004) Strength, reliability and mode of fracture of bilayered porcelain/zirconia (Y-TZP) dental ceramics.

Biomaterials, Vol. 25, pp. 5045-52, https://doi.org/10.1016/j.biomaterials.2004.02.036

[20] Fıscher J, Stawarczyk B (2007) Compability of machined Ce-TZP/Al2O3 nanocomposite and a veneering composite. Dental Materials, Vol. 23, pp. 1500-5. https://doi.org/10.1016/j.dental.2007.01.005

[21] Sailer I, Fehér A, Filser F, Lüthy H, Gauckler LJ, Schärer P, Franz Hämmerle CH (2006) Prospective clinical study of zirconia posterior fixed partial dentures: 3-year follow-up. Quintessence Internatioanal, Vol. 37, pp. 685-693.

[22] De Jager N, Pallav P, Feilzer AJ (2005) The influence of design parameters on the FEA-determined stress distribution in CAD-CAM produced all-ceramic dental crowns. Dental Materials, Vol. 21, pp. 242-251. https://doi.org/10.1016/j.dental.2004.03.013

[23] Raigrodski AJ, Chiche GJ, Potiket N, Hochstedler JL, Mohamed SE, Billiot S, Mercante DE (2006) The efficacy of posterior three-unit zirconium-oxide-based ceramic fixed partial dental prostheses: a prospective clinical pilot study. Journal of Prosthetics Dentistry, Vol. 96, pp. 237-244. https://doi.org/10.1016/j.prosdent.2006.08.010

[24] Von Steyern PV, Carlson P, Nilner K (2005) All-ceramic fixed partial dentures designed according to the DC-Zirkon technique. A 2-year clinical study. Journal of Oral Rehabilitation, Vol. 32, pp. 180-187, https://doi.org/10.1111/j.1365-2842.2004.01437.x

Ref.:
Soygun, Koray – **Özer**, Zafer – **Kurtoglu**, Cem – **Mamedov**, Amirullah M. – **Ozbay**, Ekmel: *Observation of shear bond strength between zirconia core and silica based composite material; a finite element analysis*
Építőanyag – Journal of Silicate Based and Composite Materials, Vol. 74, No. 2 (2022), 46–52. p.
https://doi.org/10.14382/epitoanyag-jsbcm.2022.7

Geotechnical properties of lateritic soil stabilized with lignocellulosic biomass fly ash

Ezenwa C. AMANAMBA ▪ Department of Civil Engineering, Abia State University, Uturu, Nigeria ▪ amanamba.ezenwa@abiastateuniversity.edu.ng

Prince ORJI ▪ Seasons Farms Limited, Nigeria ▪ princeorji40@gmail.com

Anthony EKELEME ▪ Department of Civil Engineering, Abia State University, Uturu, Nigeria ▪ chytony4real09@gmail.com

Chukwuneduzor CHIOKE ▪ Department of Building and Woodwork Technology Education, Federal College of Education (Technical), Umunze, Nigeria ▪ educhioke@gmail.com

Nnamdi NWASUKA ▪ Department of Mechanical Engineering, Abia State University, Uturu, Nigeria ▪ daddynnam@gmail.com

Érkezett: 2021. 05. 29. ▪ Received: 29. 05. 2021. ▪ https://doi.org/10.14382/epitoanyag-jsbcm.2022.8

Ezenwa C. AMANAMBA
He is a lecturer in Abia State University, Uturu, Nigeria. His research interests include highway pavement materials, transport planning and operation. He is a member of several professional bodies.

Prince ORJI
He is the Chief Operations Officer of Seasons farm limited, an agricultural economist whose research interest is in finding alternative uses for agricultural wastes.

Anthony EKELEME
He is a senior lecturer at Abia State University, Nigeria, and an adjunct lecturer at Gregory University, Uturu, Nigeria. His research interests are water resources and environmental engineering; recently he has been working on sustainable materials used in construction, to protect the environment.

Chukwuneduzor CHIOKE
He is a lecturer in Federal College of Education, Umunze, Nigeria. He has lots of industry experience in construction. He is currently a post graduate student.

Nnamdi NWASUKA
He is a lecturer in mechanical engineering at Abia State University, Nigeria, with a background in agricultural engineering. His research interests involve studies that incorporate knowledge of agricultural products and processes in the various aspects of engineering. He is currently the chairman of the Umuahia branch of the Nigeria Society of Engineers.

Abstract

This study considered the need for sustainable road construction using recycled materials. Lignocellulosicbiomass fly ash (LcBFA) gotten from Berlinia Grandiflora (Vahl) Hutch. & Dalziel (Ububa tree, in common Nigerian parlance) was used to stabilise a soil sample characterised as A-2-7 soil. The LcBFA was added to the lateritic soil at varying proportions of 0%, 10%, 20%, 30% and 40%. Chemical characterization of the LcBFA was obtained; particle size analysis, moisture content test, atterberg limit test, proctor compaction test, California bearing ratio value (CBR) test, and specific gravity test were conducted on the soil sample. The results showed an increase in plasticity, an increase in maximum dry density, a decrease of optimum moisture content and an increase in CBR value. It was concluded that LcBFA lacks the potential of serving as a pozzolan.

Keywords: LcBFA, pozzolan, wood ash, stabilization, biomass fly ash

Kulcsszavak: LcBFA, puccolán, fahamu, stabilizálás, biomassza pernye

1. Introduction

Soil is a naturally occurring organic material with such mechanical properties that makes it amenable to handling for several construction works; in this case, for several pavement layers except for the wearing course. Soil properties vary with time, location, environmental conditions, and other manmade conditions which could alter its engineering properties.

Laterite occurs as highly weathered material, rich in secondary oxides of aluminium and iron, or both [1-4]. Laterite typically has no reasonably constant property that could enable it have a generic description; in the temperate regions, laterite could be described as a red friable clayeymaterial, in the hilly tropical regions, it could be described as a tough homogenous vesicular massive material with a framework of red hydrated ferric oxides, could exist as a tough or soft coarse angular red material in the less hilly tropical regions [5].

Early studies on geotechnical properties and field performance of laterite tended to present laterite as inferior aggregates or troublesome pavement materials [6,7]; however, from extensive study on laterite, it is known that in the use of laterite for road construction, attention is paid in recognizing and utilizing the good and eliminating the poor samples, then the intermediate ones could be improved. The improvement on these intermediate ones is known as stabilization.

Soil stabilization results in increased strength, reduced compressibility, reduced permeability, or improved ground water condition [8-10]. Over the years, cement and lime stabilization have been commonly employed for improving soil properties [11-13]; these materials have rapidly increased in price due to sheer increase in the cost of energy [14].

For sake of protecting the environment and developing more sustainable pavement materials, several admixtures have been explored, most interestingly from solid wastes. Ideally, the availability of these eco-friendly binders will never diminish considering that human activity will continue; hence, a constant release of solid wastes, that can be conveniently utilized for pavement construction, instead of constituting challenges to public health experts [10]. Several materials which would have been considered solid wastes have, over the years, been researched and explored as partial replacement for lateritic soils. Some of these materials include: fly ash, rice husk ash, snail shell ash, oyster shell powder, waste tire ash, palm oil fuel ash, quarry dust, coffee husk ash, biomass ash, paper ash, egg shell ash, crushed waste ceramics, crushed waste glass, bagasse ash, palm fibre, crushed waste plastics, palm kernel shell ash, periwinkle shell ash, bio-peels, sawdust, biochar, iron ore tailings, glass fibre, metallurgical slag, etc. [10]. In some cases, these materials have been used as admixtures for other pavement materials other than soil; [15] explored the use of fly ash and crushed glass wastes for improving asphalt.

Most commonly, fly ash from coal fired-furnaces, municipal solid wastes (MSW) and wood ash have been extensively researched, especially for easy adaptation in low- and middle-income countries like Nigeria where flexible pavement failure has become common [16]. Use of MSW and wood ash for soil stabilization can be considered more relatable owing to the fact that while fly ash is a by-product of an industrial process, MSW is a function of daily activities of man, and wood is commonly used as biomass, and sometimes the wood ash from such process constitutes municipal wastes.

[17] studied the reuse of municipal solid waste (MSW) ash as an admixture in the stabilization of a soft marine clay. This resulted in more than 75 times improvement in strength of untreated clay, and improvement in drainage property. However, [18] considered the advantages of municipal solid wastes incineration (MSWI) in highway engineering alongside its negative environmental impacts, especially leaching of heavy metals into the in-situ soil; the study concluded that while these downsides exist, the reduction in construction costs following the use of MSWI and the reduction in municipal wastes in developing countries are huge advantages. Agreeing with the merits of use of MSWI in pavement construction, [19] concluded that there is a potential efficiency of municipal waste disposal, making them reusable materials as eco-friendly binders with zero carbon emission and consequently reduced contribution to global warming.

[20] considered the use of wood ash as a pozzolan, in the stabilization of clay. It was found that there were improvements in the engineering properties of existing soil particularly in terms of compaction, shear strength parameters, unconfined compressive strength (UCS), workability, and compressibility.

In a similar study, [21] found that the Optimum Moisture Content (OMC) of the study soil increased while Maximum Dry Density (MDD) decreased and California Bearing Ratio (CBR) increased; hence, concluding that the addition of wood ash as a pozzolan had positive impacts on the strength characteristics of the study soil sample.

This paper considered the use of lignocellulosic biomass fly ash (LcBFA) as a stabilizing agent. In order to reduce the cost implications of the commonly applied soil additives, and to utilize readily available alternatives, LcBFA derived from wood has been selected for this research. Wood is a naturally occurring material obtained from trees, the end product of these trees when burnt in the course of cooking is LcBFA; this generally, has a pozzolanic property which alters most properties of soil that makes it become suitable for construction [5,22].

2. Materials and methods

Wood from *Berlinia Grandiflora (Vahl) Hutch. & Dalziel* (Ububa tree, in common Nigerian parlance) was used to generate LcBFA. The tree is very common in Africa, and has several uses, ranging from construction to medico-ethnobotanical uses [23]. The LcBFA sample used was gotten from Jokwa bakery oven in Afikpo, Afikpo-North L.G.A, Ebonyi state, Nigeria. This bakery uses wood pieces from Ububa tree were used for heating up the oven. The sample obtained was black in colour, an indication of high carbon content; it was sundried for 3 days and stored in polyethylene bags. Only fractions passing BS sieve No. 200 (75 μm) was used throughout the test without additional treatment.

Lateritic soil sample was taken from palm plot borrow pit which is located in Unwana, Afikpo-North Local Government Area of Ebonyi State, Nigeria. The climate in the area is tropical with alternating rainy and dry seasons. The borrow pit lies on latitude 5°51'45.0"N and longitude 7°56'55.0"E, and elevation of 107m above sea level. The disturbed sample was collected, slightly pulverized with minimal pressure to break up lumps in order to facilitate air drying, sundried for 3 days and readied for use.

3. Experimental programme

In accordance with BS1377 Methods of Test for Soils for Civil Engineering Purposes [24], and BS 6031 Codes of practice for earth works [25], various tests were carried out on the control sample (sample with 0% fly ash). Thereafter, soil sample was mixed with LcBFA in gradual additions by percentage (10%, 20%, 30% and 40%) of the total weight of the sample used; this was manually done. Subsequently, soil tests were carried out at repeated intervals, on the soil sample mixed with LcBFA.

Chemical characterization of the LcBFA was obtained, particle size analysis, moisture content test, atterberg limit test,proctor compaction test, California Bearing Ratio value (CBR) test, and specific gravity test were conducted on the control soil sample to characterize it, then CBR and proctor compaction tests were repeated to check the effect of LcBFA on the soil sample.

4. Results and discussion

4.1 Control sample

The sample soil was categorised following the American Association of State Highway and Transportation Officials (AASHTO) classification standards as A-2-7 soil, considering that the gradation curve has more distribution in the third segment of the major gridlines of x-axis and the values of the liquid limit and plasticity index; thus, showing properties of fair soil for pavement construction. A summary of the properties of the lateritic soil is presented in *Table 1* and *Fig.1*below.

Parameter	Values
NMC (%)	12.21
LL (%)	27.08
PL (%)	16.04
PI (%)	11.04
OMC	16
MDD	1.63
CBR	49.8
S.G	2.67

Table 1 Properties of soil sample
1. táblázat A talajminta tulajdonságai

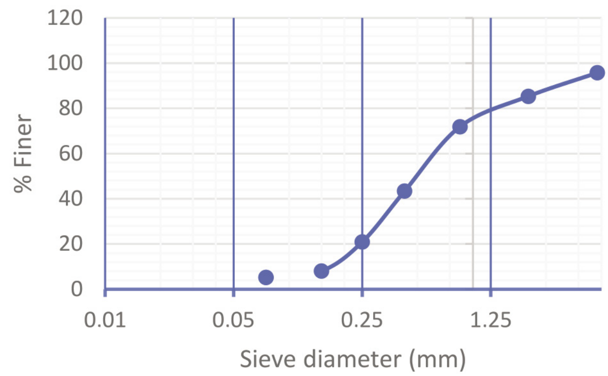

Fig. 1 Gradation curve of soil sample
1. ábra Talajminta szemeloszlási görbéje

4.2 LcBFA

Several standards suggests that a material like ash can be considered to be a pozzolan if the composition of $SiO_2+Al_2O_3+Fe_2O_3$is greater or equal to 70%[9,26]. In this case, as shown in *Table 2*, the percentage composition of aluminosilicates is just 61.58%; though, slightly less than the specified standard, it cannot be considered a pozzolan.[27-29] demonstrated that the pozzolanic activity of a material is dependent on its high aluminosilicate contents, especially SiO_2.

Constituent	SiO_2	Al_2O_3	Fe_2O_3	CaO	MgO	Na_2O	K_2O
Percentage	32.30	27.00	2.28	10.73	9.25	6.70	10.40

Table 2 Chemical composition of LcBFA
2. táblázat LcBFA kémiai összetétele

4.3 Addition of LcBFA to soil sample

The gradual addition of LcBFA to the borrow pit soil sample yielded some positive results with respect to compressibility and strength of the soil.

The atterberg limit tests were repeated for Run 1 (0% LcBFA), Run 2 (10% LcBFA), Run 3 (20% LcBFA), Run 4 (30% LcBFA) and Run 4 (40% LcBFA). From *Fig. 2*, it can be seen that LL values increased gradually, the PL values decreased but at a rate faster than the increase of the LL, and the PI increased a bit more abruptly.

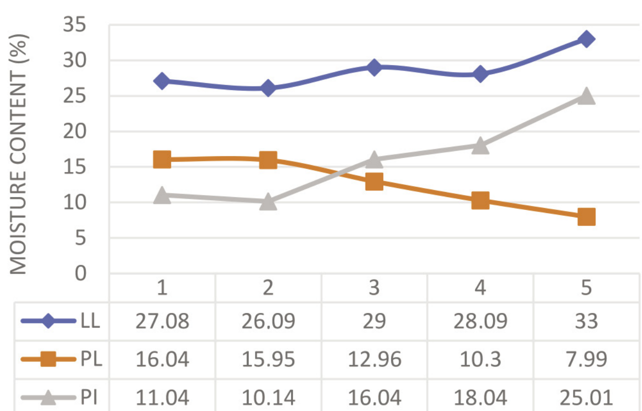

Fig. 2 Plot of Atterberg limit values
2. ábra Atterberg határértékek

The effect of the LcBFA was monitored as the ratio of the soil:LcBFA was gradually altered from 100%:0% to 60%:40%. From *Fig.3*, it can be seen that OMC increased from 0% addition of the LcBFA to 10% addition of the LcBFA, subsequently, the OMC decreased until 12.2% at 40% addition of LcBFA. Conversely, the MDD constantly increased from 1.63g/cm³ at 0% addition of the LcBFA to 1.96g/cm³ at 40% addition of the LcBFA.

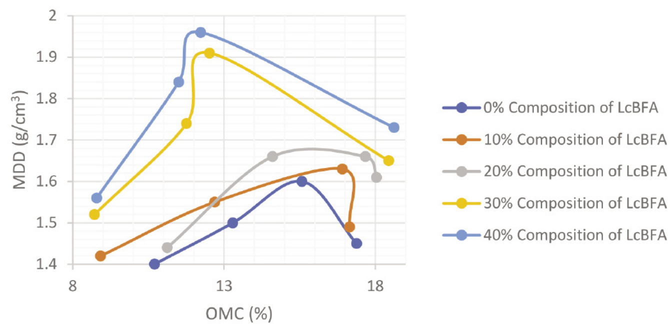

Fig. 3 Plot of proctor compaction test results
3. ábra Proctor tömörítési vizsgálati eredmények

Lastly, it was observed that the CBR values increased gradually with a gradual increase in the proportion of the LcBFA added to the soil sample. The obtained CBR values have been presented in figure 4 below.

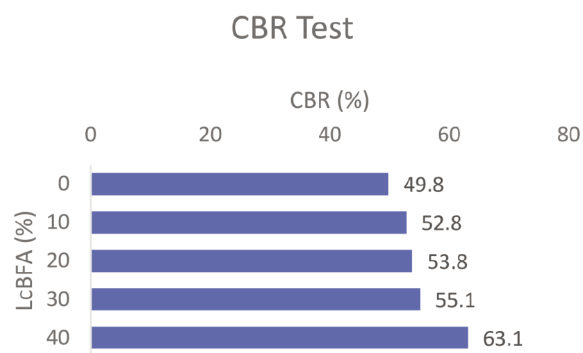

Fig. 4 CBR test results
4. ábra CBR vizsgálati eredmények

5. Conclusions

This study presented several test results conducted, to evaluate the effect of LcBFA on an A-2-7 soil. From the results obtained, the study concludes thusly:

As opposed to the use of other pozzolans as stabilizing agent, LcBFA increased the PI of the soil sample. This could be explained by the fact that the increase in the LcBFA, increased the composition of fine particles in the soil sample, without a commensurate pozzolanic activity to cement the materials.

The MDD was found to be on the increase as OMC decreased. This could be attributed to the nature of the soil sample. In agreement with the findings of other studies.

There was an increase in the CBR value of the soil sample. While there is a possibility that this can be attributed to the chemical composition of LcBFA, generally, the introduction of finer particles in A-2-7 should improve gradation and soil strength.

Lastly, the chemical composition of the LcBFA suggests that it is not a pozzolan. The pozzolanic activity of an admixture causes a reaction that converts a silica-rich material with no cementing properties, to a calcium silicate, which is characterised by good cementing properties. Unlike most pozzolans from waste materials, like rice husk ash, fly ash and sugarcane bagasse with significant SiO_2 proportions, ranging from 67.3% [32], 55.0% [33], and 64.38% [34] respectively, LcBFA has SiO_2 of just 32.3% as determined in this research. The findings here are in agreement with the argument of several other studies. The use of biomass fly ash as a pozzolan is dependent on its chemical composition; hence, with this understanding and other issues raised above, it is safe to say that LcBFA is not a pozzolan.

References

[1] Maigien, R. (1966) Review of Research on Laterites. Natural Resources Research IV. *United Nations Educational Scientific and Cultural Organization (UNESCO)*, Paris.

[2] Gidigasu, M. D. (1976) Laterite Soil Engineering. *Elsevier Scientific Publishing Co.*, New York.

[3] Charman, J. H. (1988) Laterite in Road Pavements, Special Publication 47. *Construction Industry Research and Information Association (CIRCA)*, Westminster, London.

[4] Amadi, A. (2010) Evaluation of Changes in Index Properties of Lateritic Soil Stabilized with Fly Ash. *Leonardo Electronic Journal of Practices and Technologies*. Vol. 17, 2010, pp.69 – 78

[5] Amu, O., Adewumi, I. K., Ayodele, A. L., Mustapha, R. A., Ola, O. O. (2005) Analysis of California Bearing Ratio Values of Lime and Wood Ash Stabilized Lateritic Soil. *Journal of Applied Sciences.*Vol. 5, No. 8, 2005, pp.1479 – 1483

[6] Terzaghi, K., Robertson, R. H. S. (1958) Design and performance of the sasumua dam. *Proceedings of the Institution of Civil Engineers.*Vol. 9, No. 4, 1958, pp.369-394

[7] Nanda, R. L., Krishnamachari, R. (1958) A study of soft aggregates from different parts of India with a view to their use in road construction. *Central Road Resources Institute,* India.

[8] Elmashad, M. E., Hafez, N. M. (2017) Sand Biogrouting through the deposition of Calcium Carbonate by Ureolytic Bacteria. *Journal of scientific and Engineering Research.*Vol. 4, No. 7, 2017, pp.377-382

[9] Onyelowe, K. C., Onyia, M. E., Van, D. B., Baykara, H., Ugwu, H. U. (2021) Pozzolanic reactions in clayey soils for stabilization purposes: A classical overview of sustainable transport geotechnics. *Advances in Materials Science and Engineering*. 2021, pp.1 – 7, https://doi.org/10.1155/2021/6632171

[10] Onyelowe, K. C., Van, D. B., Ubachukwu, O., Ezugwu, C., Salahudeen, B., Van, M. N., Ikeagwuani, C., Amhadi, T., Sosa, F., Wu, W., Duc, T. T., Eberemu, A., Duc, T. P., Barah, O., Ikpa, C., Orji, F., Alaneme, G., Amanamba, E., Ugwuanyi, H., Sai, V., Kadurumba, C., Subburaj, S., Ugorji, B.(2019) Recycling and reuse of solid wastes; a hub for ecofriendly, ecoefficient and sustainable soil, concrete, wastewater and pavement reengineering. *International Journal of Low-Carbon Technologies*. Vol. 14, No. 3, September 2019, pp.440–451, https://doi.org/10.1093/ijlct/ctz028

[11] Prusinski, J. R., Bhattacharja, S. (1999) Effectiveness of Portland Cement and Lime in Stabilizing Clay Soils. *Transportation Research Record*. Vol. 1652, No. 1, 1999, pp.215-227, https://doi.org/10.3141/1652-28

[12] Sherwood, P. T. (1995) Soil Stabilization with Cement and Lime, Rev. Ed. *TRL*, Crowthorne.

[13] Onyelowe, K. C. (2012) Geochemistry of Soil Stabilization. *ARPN Journal of Earth Sciences.*Vol. 1, No. 2, 2012, pp.32-35

[14] Neville, A. M. (2000) Properties of Concrete, 4th Edition. *Longman*, Malaysia.

[15] Onyelowe, K. C., Onyia, M., Onukwugha, E. R., Van, D. B., Obimba-wogu, J., Ikpa, C. (2020) Mechanical properties of fly ash modified asphalt treated with crushed waste glasses as fillers for sustainable pavements. *Epitoanyag - Journal of Silicate Based & Composite Materials.*Vol. 72, No. 6, 2020, pp.219-222, https://doi.org/10.14382/epitoanyag-jsbcm.2020.35

[16] Amanamba, E. C., Chioke, C., Ekeleme, A. C. (2021) Evaluation of the causes of flexible pavement failure: case study of Enugu/Port Harcourt Expressway. *Nigerian Journal of Technology*, 2021

[17] Show, K., Tay, J., Goh, A. T. C. (2003) Reuse of incinerator fly ash in soft soil stabilization. *Journal of materials in civil engineering.*Vol. 15, No. 4, 2003, https://doi.org/10.1061/(ASCE)0899-1561(2003)15:4(335)

[18] Lu, Y., Tian, A., Zhang, J., Tang, Y., Shi, P., Tang, Q., Huang, Y. (2020) Physical and Chemical Properties, Pretreatment, and Recycling of Municipal Solid Waste Incineration Fly Ash and Bottom Ash for Highway Engineering: A Literature Review. *Advances in Civil Engineering*. 2020, pp.1 – 17, https://doi.org/10.1155/2020/8886134

[19] Onyelowe, K. C. (2018) Soil Stabilization and the Synthesis and Application of Nanostructured Ash from Biomass and Municipal Solid Wastes for a Green Environmental Geotechnics. *3rd international nanotechnology conference and expo*, Rome, Italy; 7-9 May, 2018

[20] Nath, B. D., Sarkar, G., Siddiqua, S., Rokunuzzaman, M., Islam, M. R. (2018) Geotechnical Properties of Wood Ash-Based Composite Fine-Grained Soil. *Advances in Civil Engineering*. 2018, pp.1 – 7, https://doi.org/10.1155/2018/9456019

[21] Abdulwahab, R., Ibitoye, B. A., Akinleye, M. T., Ahmed, N. T. (2018) The Effects of Wood ash on the Geotechnical Properties of Lateritic Soil. *USEP: Journal of Research Information in Civil Engineering.*Vol. 15, No. 1, 2018, pp.1986 – 1995

[22] Okagbue, C. O. (2007) Stabilization of Clay Using Wood Ash. *Journal of Materials in Civil Engineering.*Vol. 19, No. 1, 2007, https://doi.org/10.1061/(ASCE)0899-1561(2007)19:1(14)

[23] Uzodimma, D. E. (2013) Medico-ethnobotanical inventory of Ogii, Okigwe Imo state, south eastern Nigeria. *Global Advanced Research Journal of Medicinal Plants.*Vol. 2, No. 2, 2013, pp.30 – 44

[24] British Standards Institute (1990). BS 1377: 1990. Methods of Test for Soils for Civil Engineering Purposes. *British Standards Institute*, London.

[25] British Standards Institute (2009). BS 6031:2009 Code of Practice for Earthworks. *British Standards Institute*, London

[26] Alp, İ., Deveci, H., Süngün, Y. H., Yilmaz, A. O., Kesimal, A., Yilmaz, E. (2009) Pozzolanic characteristics of a natural raw material for use in blended cements. *Iranian Journal of Science & Technology, Transaction B, Engineering*. Vol. 33, No. B4, pp 291-300

[27] Papadakis, V. G.,Tsimas, S. (2002). Supplementary materials in concrete. Part I: Efficiency and design. *Cement and Concrete Research*. Vol. 32, 2002, pp. 1035-1041, https://doi.org/10.1016/S0008-8846(02)00827-X

[28] Papadakis, V. G., Antiohos, S.,Tsimas, S. (2002). Supplementary materials in concrete. Part II: A fundamental estimation of the efficiency factor. *Cement and Concrete Research*. Vol. 32, 2002, pp. 1533-1538, https://doi.org/10.1016/S0008-8846(02)00829-3

[29] Sideris, K. K., Savva, A. E.,Papayianni, J. (2006). Sulfate resistance and carbonation of plain and blended cements. *Cement and Concrete Composites*. Vol. 28, 2006, pp. 47–56, https://doi.org/10.1016/j.cemconcomp.2005.09.001

[30] Solihu, H. (2020) Cement soil stabilization as an improvement technique for rail track subgrade, and highway subbase and base courses: A review. *Journal of Civil and Environmental Engineering.*Vol. 10, No. 3, 2020, pp.1-6

[31] Oluremi, J.R., Elsaigh, W.A., Ikotun, B.D., Osuolale, O. M., Adedokun, S. I., Oyelakin, S. E., Ayodele, O. P. (2021) Strength enhancement in high silica wood ash stabilized lateritic soil using sodium tetraoxosulphate VI (Na2SO4) as activator. *International Journal of Pavement Research Technology*. Vol. 14, 2021, pp.410–420, https://doi.org/10.1007/s42947-020-0087-2

[32] Oyetola, E.B.,Abdullahi, M. (2006). The use of rice husk ash in low-cost sandcrete block production. *Leonardo Electronic Journal of Practical Technology*. Vol. 8, 2006, pp.58-70.

[33] Brookes, R. M. (2009) Soil stabilization with flyash and rice husk ash. *International Journal of Research and Reviews in Applied Sciences.*Vol. 1, No. 3, 2009, pp.209 – 217

[34] Kharade, A. S., Suryavanshi, V. V., Gujar, B. S., Deshmukh, R. R. (2014) Waste product 'bagasse ash' from sugar industry can be used as stabilizing material for expansive soils. *International Journal of Research in*

Engineering and Technology.Vol. 3, No. 3, 2014, pp.506-512
[35] Abdullahi, M. (2006) Characteristics of wood ash/OPC concrete. *Leonardo Electronic Journal of Practical Technology*. Vol. 8, 2006, pp.9–16.
[36] Teixeira, S.R.,De Souza, A.E.,De Almeida Santos, G.T., Vilche Peña, A.F., Miguel, A.G. (2008) Sugarcane bagasse ash as a potential quartz replacement in red ceramic. *Journal of the American Ceramic Society*. Vol. 91, 2008, pp.1883–1887, https://doi.org/10.1111/j.1551-2916.2007.02212.x
[37] American Coal Ash Association (1995) Fly Ash Facts for Highway Engineers.*American Coal Ash Association*, Colorado
[38] Grau, F., Choo, H., Hu, J. W., Jung, J. (2015) Engineering Behaviour and Characteristics of Wood Ash and Sugarcane Bagasse Ash. *Materials*. Vol. 8, No. 10, 2015, pp.6962-6977, https://doi.org/10.3390/ma8105353
[39] Barišić, I., NetingerGrubeša, I., Dokšanović, T., Marković, B. (2019) Feasibility of Agricultural Biomass Fly Ash Usage for Soil Stabilisation of Road Works. *Materials*. Vol. 12, No. 9, 2019, pp.1375, https://doi.org/10.3390/ma12091375
[40] Sarkkinen, M., Kujala, K., Kemppainen, K., Gehor, S. (2016) Effect of biomass fly ashes as road stabilisation binder. *Road Materials and Pavement Design*. Vol. 19, No. 1, 2016, pp.239-251, https://doi.org/10.1080/14680629.2016.1235508

Ref.:
Amanamba, Ezenwa C. – **Orji**, Prince – **Ekeleme**, Anthony – **Chioke**, Chukwuneduzor – **Nwasuka**, Nnamdi: *Geotechnical properties of lateritic soil stabilized with lignocellulosic biomass fly ash*
Építőanyag – Journal of Silicate Based and Composite Materials, Vol. 74, No. 2 (2022), 52–56. p.
https://doi.org/10.14382/epitoanyag-jsbcm.2022.8

Band structures of metacomposite based phononic crystals in quasi-Sierpinski fractals

Oral OLTULU ▪ Department of Physics, Faculty of Sciences, Harran University, Turkey ▪ oltulu@harran.edu.tr
Zafer OZER ▪ Mersin Vocational High School Electronic and Automation Department, Mersin University, Turkey ▪ zaferozer@mersin.edu.tr
Amirullah M. MAMEDOV ▪ Nanotechnology Research Center (NANOTAM), Bilkent University, Turkey ▪ International Scientific Center, Baku State University, Azerbaijan ▪ mamedov46@gmail.com
Ekmel OZBAY ▪ Nanotechnology Research Center (NANOTAM), Bilkent University, Turkey ▪ ozbay@bilkent.edu.tr

Érkezett: 2021. 05. 29. ▪ Received: 29. 05. 2021. ▪ https://doi.org/10.14382/epitoanyag-jsbcm.2022.9

Oral OLTULU
Prof. of Department of Physics, Faculty of Arts and Sciences, Harran University. Conducts research on materials, photonics crystals and phononic crystals.

Zafer ÖZER
Assoc. Prof. of Department of Automation and Electronics, Mersin Vocational High School, Mersin University. Conducts research on materials, photonics crystals and phononic crystals.

Amirullah M. MAMEDOV
Prof. of NANOTAM, Nanotechnology Research Center, Bilkent University. Conducts research on physico-mechanical properties of materials and metamaterials.

Ekmel OZBAY
Prof. of NANOTAM, Nanotechnology Research Center, Bilkent University. Conducts research on materials and metamaterials.

Abstract
In this paper, we investigated the bandgaps of two-dimensional phononic crystals with quasi-Sierpinski carpet unit cells in a metacomposite based solid–solid phononic crystal. Finite element method was used to analyze the properties of two-dimensional phononic bandgaps (2D PBGs) in a quasi-fractal structure. Two new types of quasi-Sierpinski fractal unit cells whose constituents are homogeneous and isotropic were proposed to obtain larger full bandgaps. The results show that the PBGs of the proposed quasi-Sierpinski fractals are suitable to tune the PBG's without changing the size of the phonic crystal. The new quasi-Sierpinski fractals also retain the self-similarity as in the third-order Sierpinski fractal unit cell. The investigated quasi-fractals can be easily modified to increase the filling fraction of the constituents, which can be effectively used to enlarge existing PBG by preserving degree of self-similarity structure.
Keywords: phononic crystals, metacomposite, quasi-Sierpinski carpet, bandgaps
Kulcsszavak: fononikus kristályok, metakompozit, kvázi-Sierpinski szőnyeg, sáv hézagok

1. Introduction

When an elastic wave propagates through periodic solid structures, a unique feature of periodic structures may be exhibited as phononic bandgaps (PBGs). Elastic waves with frequencies in the band gap ranges cannot propagate in the periodic structures. The existence and location of bandgaps are dependent on the material and geometrical parameters of the representative unit cell. The location and spatial distribution of bandgaps are dependent on the material, structural optimization, topology optimization, and geometrical parameters of the representative unit cell. Recently, some interesting behaviors by fractal configurations (Sierpinski carpet and Sierpinski gasket) have been discovered by researchers in recent years [1-4]. Generally, fractal systems, over microscopic to macroscopic length scales, are ubiquitous in nature. Inspired by the natural fractal, hierarchical structures/ composites with self-similar fractals have been de-signed for achieving remarkable mechanical properties (high stiffness, strength, toughness). Besides the fractal- inspired hierarchical structures, periodic structures (well-known as phononic crystals) aiming at modulating wave propagation have received growing interests in the latest decade. For a phononic crystal, the frequency range within which the incident wave with any propagation direction cannot pass through is deemed to be a bandgap. It provides guidance for the design of the acoustic filter and the sound/vibration insulator by investigating the band structure of a phononic crystal [1].

Due to the unique features of fractal structures [3], most of the studies have been focused on developing strategies to obtain low, high, and wider frequency bandgaps by changing the fractal order and fractal size. However, it is a difficult task to change the distinctive characteristic of the wave propagation with the traditional Sierpinski fractals. Therefore, ongoing studies have been shifted to quasi-fractal phononic crystals to broaden the potential applications in the field of noise control and vibration reduction.

Yan et al. proposed layered phononic crystals with different fractal super-lattices and studied elastic wave localization in them [4]. Gao and Wu et al. investigated the bandgaps of two-dimensional (2D) PCs which are constituted by self-similarity shape cells [5, 6]. Norris used the finite-difference time-domain (FDTD) analysis to determine the impact of periodic fractal-shaped inclusions on the frequency response of 2D PCs. [7]. Kuo and Piazza introduced the T-square fractal geometry design for a microscale phononic BG structure in aluminum nitride and obtained ultra-high frequency bandgaps by the design of fractal phononic crystals in aluminum nitride [8, 9]. Liu et al. presented T-square fractal holes in a solid/air structure and found the origin of the lower frequency bands [10].

The PCs with periodically distributed void pores belong to a kind of light weight structure. Wang has studied the bandgap of the 2D PC with a kind of nonconvex holes [11]. Liu has studied the influence of T-square fractal shape holes on the band structure of 2D PCs [12]. This research shows that the structure with increasing fractal level of the holes results will affect the BGs.

Gao et al. obtained low-frequency BGs by studying the effects of the geometrical parameters and degree of the self-similarity structure [13].

In order to study the impact of a quasi-fractal design on the band structures of the two-dimensional phononic crystal, we propose two new types of quasi-fractal unit cells were to obtain large full bandgaps by designing two different quasi-Sierpinski carpet unit cells.

2. Unit cell with fractal pattern

We consider a type of two-dimensional metacomposite phononic crystal with its unit cell consisting of a fractal Sierpinski gasket structure. The structure is distributed in a square array with the lattice constant *a*. Therefore, we start with a square plate, as illustrated in *Fig. 1(a)*. Geometrically, the Sierpinski carpet structure that exhibits a repeating pattern at every level is a fractal topological structure. If the repeated pattern is the same as the previous one, self-similarity appears in the structure. However, a self-similar pattern in the structure at each level has a different scaling factor for the fractals with various degrees of self-similarity. In the Sierpinski gasket structure, the unit square with lattice constant a is equally divided into 9 sub squares that make up a 3×3 array of sub cells, as shown in *Fig. 1(b)*. From the array, a small central square of side length b is carved out from an elastic matrix and filled with the other material of choice. At this step, the second-order fractal, *n*=2, whose side length *a*/3 is obtained. Repetition of this process for the remaining sub squares gives Sierpinski carpet structure with *n*=3, as shown in *Fig. 1(c)*. It is seen that the side length of the unit square is reduced by 1/3 for the second-order. Applying the same rule at each iteration, subcells of lateral size $b_n = a \times (1/3)^{n-1}$ can be obtained. Briefly, the Sierpinski fractal unit cells with first-order (*n*=1), second-order (*n*=2), third-order (*n*=3), and fourth-order (*n*=4) are given in *Fig. 1(a)-(d)*, respectively. It is clear that a square structure with its side length is considered as the first-order fractal.

The fourth-order Sierpinski Carpet can be used to obtain a quasi-Sierpinski carpet. Therefore, some modifications to the fourth order Sierpinski structure can be made in order to get a new quasi-Sierpinski carpet. However, in order to attain a wider frequency band gap, modifications are employed in two different ways to utilize two new types of quasi-Sierpinski carpets. The first quasi-Sierpinski fractal structure was obtained by only connecting the squares with a side lenght of $a_o/27$ around the squares with a side lenght of $a_o/9$. *Fig. 2 (a)* and *(b)* show the example of a quasi-fractal structure and its pattern formation.

On the other hand, the second quasi-Sierpinski fractal structure was also obtained by only connecting the squares with a side lenght of $a_o/27$ along the *x* and *y* direction in a way that no sides of any other squares with a side lenght of $a_o/3$ and $a_o/9$ were cut through. *Fig. 3(a)* and *(b)* show the example of a quasi-fractal structure and its pattern formation.

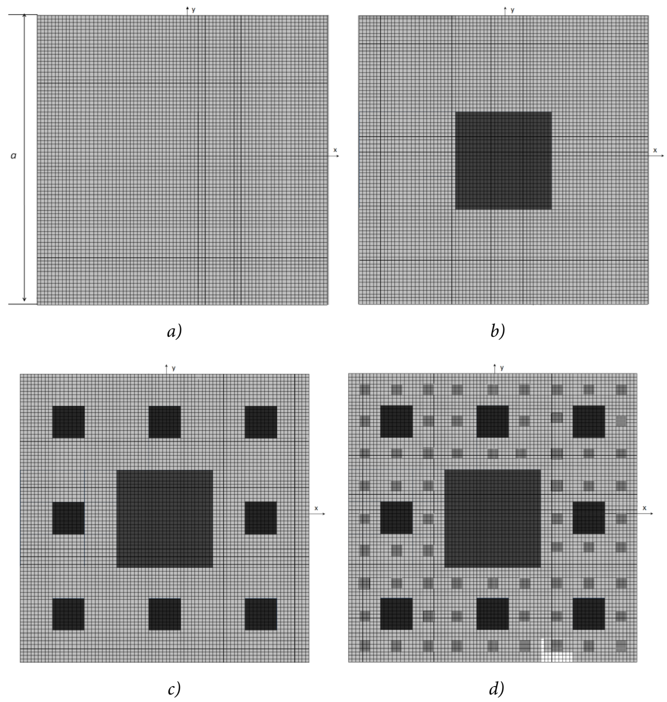

Fig. 1 Traditional Sierpinski-carpet unit cells with first-order (a), second-order (b), third-order (c) and fourth-order (d, respectively)
1. ábra Elsőrendű (a), másodrendű (b), harmadrendű (c) és negyedrendű (d) hagyományos Sierpinski-szőnyeg egységcellák

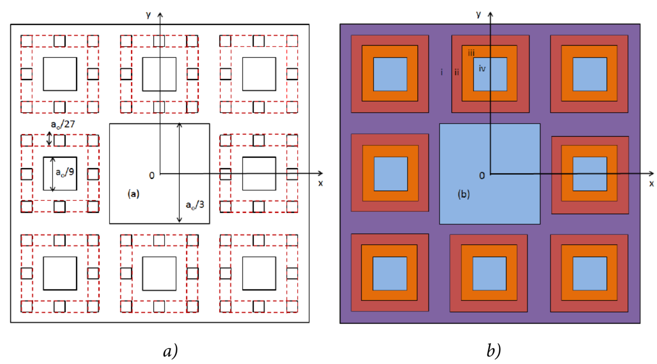

Fig. 2 Quasi-Sierpinski carpet unit cell (a) and its pattern formation (b)
2. ábra Kvázi-Sierpinski szőnyeg egység cella (a) és mintázatának kialakítása (b)

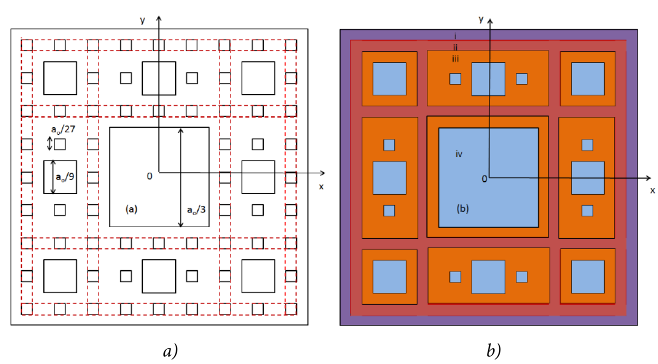

Fig. 3 Quasi-Sierpinski carpet unit cell (a) and its pattern formation (b)
3. ábra Kvázi-Sierpinski szőnyeg egység cella (a) és mintázatának kialakítása (b)

The unit cell of both quasi-Sierpinski fractal structures consists of a center square as in the 2nd order Sierpinski carpet with six other squares repeated as in the 3rd order repeating at its corners. Due to the specific placement of the square rods, these two quasi fractal structures still retain their symmetry. These particular arrangements give rise to four different regions within the structure. These four different regions are shown in *Fig. 2 (b)* and *3 (b)*. This can allow us to consider the structure as a four-component material structure. As a result of the obtained geometry, the elastic matrix was filled with four different materials. Suggesting such structures with the self-similar arrangement also show that the fractals behave as phononic quasi-crystals.

The unit cell, which comprises region I, region II, region III, and region IV, are filled with matrix material silicon rubber composite, $LiNbO_3$ inclusions, PZT($Pb[Zr_xTi_{1-x}]O_3$ - Lead Zirconate Titanate) inclusions and porous Si_3N_4 composite inclusions, are arranged in a square lattice with the lattice constant a =1.5 mm. Density ρ, Elastic modulus E, and Poisson's ratio $\boldsymbol{\nu}$ of rubber, PZT and porous Si_3N_4 composite are ρ_1=1300 kg/m^3 E_1=1.175x10^5 [Pa] ν_1=0.4688, ρ_2=11600 kg/m^3 E_2=40.819x10^9 [Pa] $\boldsymbol{\nu}_2$=0.3698 and ρ_3=17800 kg/m^3 E_3= 3.6x10^{11}[Pa] ν_3=0.28, respectively [14]. Parameters of piezoelectric material properties of PZT and $LiNbO_3$ were used as default parameters defined by the COMSOL® software.

3. Results and discussion

In order to understand the variation of the two quasi-Sierpinski carpets PBG, the Finite Element Method (FEM) based on the COMSOL® simulation software with the solid mechanics module was used to find the band structures. The bandgap structures of in-plain modes for *Fig. 2* and *3* are given in *Fig. 4(a)* and *(b)*. There are absolute bandgaps that appeared as shown in both figures along with Γ-X, Γ-M and X-M directions. *Fig. 4(a)* shows a wide full bandgap ranging from 14622.91 Hz to 25919.86 Hz. However, a larger full band gap appeared in the frequency range from 6561.301 Hz to 25032.66 Hz, *Fig. 4(b)*. Since the conventional Sierpinski carpets are difficult to significantly adjust the band gap behavior because the filling fraction is small. The difference between the full bandgaps is probably due to the increased filling ratio as well as the difference between the structures. *Fig. 4(a)* and *(b)* show that proposed the quasi-Sierpinski carpet phononic crystals have a wider and expanded vibration isolation capacity.

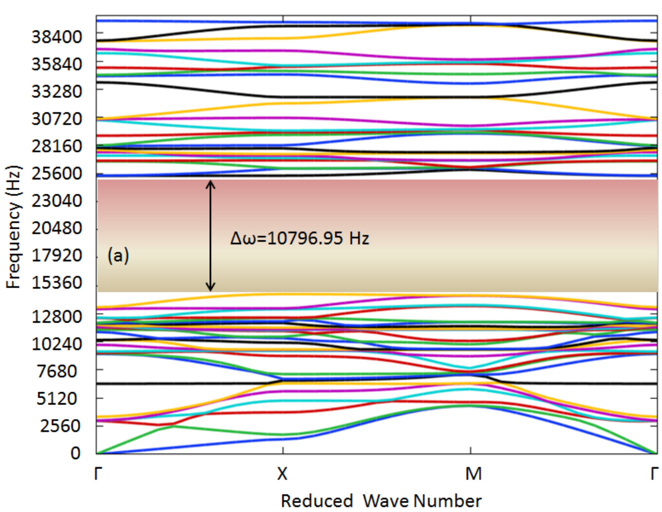

a)

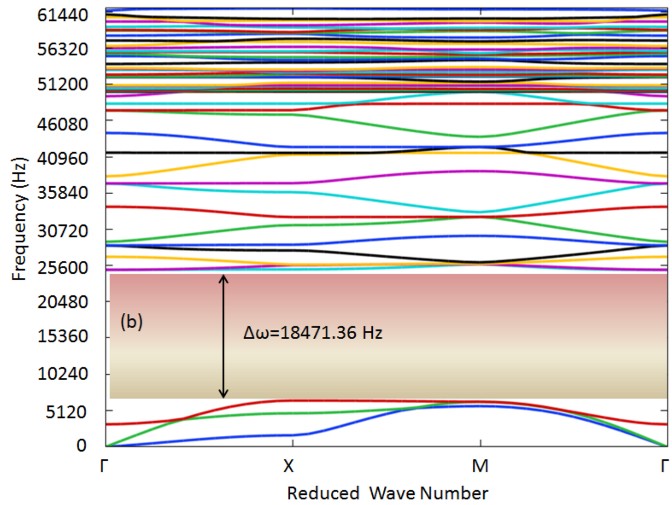

b)

Fig. 4 Band structures of the PC structures, (a) and (b), as described in Fig. (2) and (3), respectively

4. ábra A (2) és (3) ábrák szerint PC-struktúrák (a) és (b) sáv hézagai

The reflection and refraction of a certain wave can be analyzed in the space of wave numbers by considering the equifrequency surface (EFS) of the wave. This surface is described by the dispersion relation of the anisotropic medium at the fixed frequency ω. The EFSs of the incident wave along the Γ–X–M–Γ direction are shown in *Figs. 5(c-d)*. *Figures 5(s-d)* show that local curvature of the equi-frequency contours deviates from circular symmetry. The circular contours are distorted and become a rectangular-like contour by leading to a simple symmetry for values of k_x equal to k_y. An equi-frequency plot of the 2-nd band, which is a little bit complicated than the 1-st band exhibits a square-like contour. The case of a non-circular equi-frequency contour, however, indicates anisotropic behavior.

On the other hand, a square-like contour also reflects some symmetry in a particular direction. This could especially be advantageous and even be more effective if the self-collimation property of the phononic crystal is considered. It must be noted that the group velocity v_g is normal to the equi-frequency contour but not collinear to the wave vector k. At each frequency, the energy flow direction is given by the normal to the equi-frequency contour, and is in the direction of the maximum rate of change of frequencies. The calculated contours also allow us to analyze whether the phononic crystal can have negative refraction or not, depending on the sign of the dispersion slope. From the equi-frequency contour plots above, we can see that the radius of the circle increases with frequency. Hence, we can conclude that the dispersion slope is positive. In order to understand the dynamics of wave propagation, the concept of group velocity may be useful from the viewpoint of energy transportation. Therefore, the group velocity is the speed, with which a wave packet moves, along the high-symmetry directions Γ–X–M of the Brillouin zone. It is worth to mention that the group velocity of waves are zero at the some high symmetric points (X or M) meaning that there is no energy transfer at these points (*Figs. 5a* and *5b*).

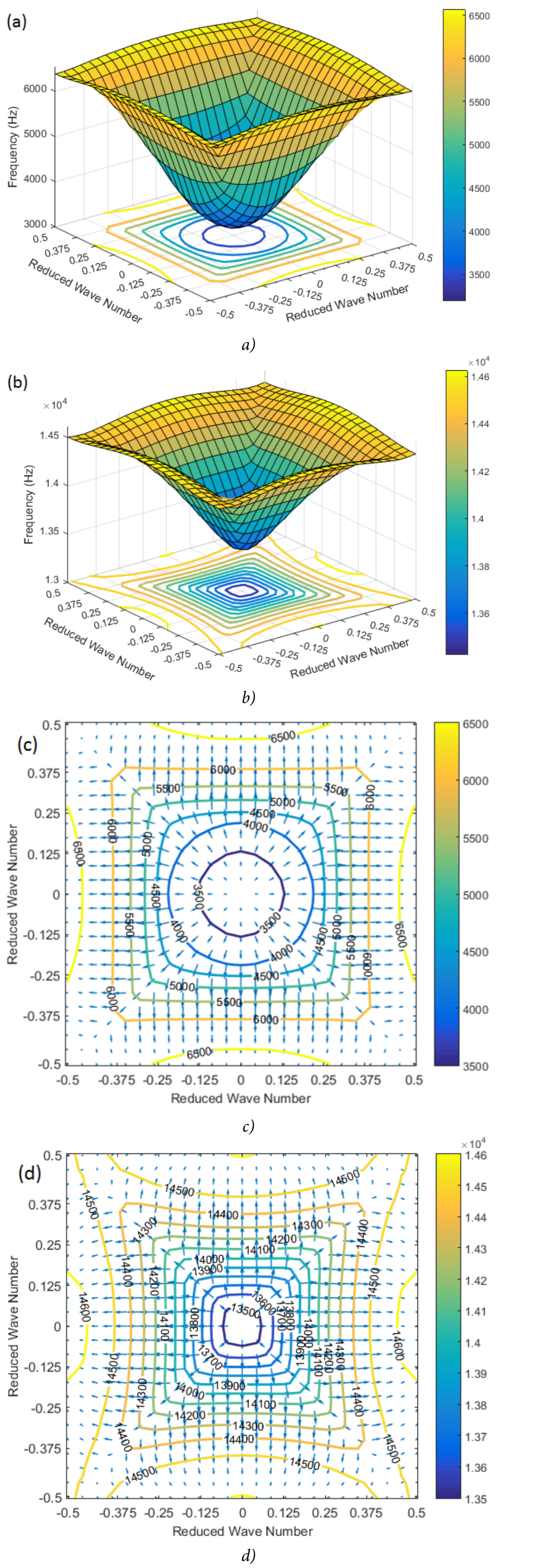

Fig. 5 The dispersion relation ω(k), for the 27th and 3rd modes for all k vectors in the first Brillouin zone, (a-b). Corresponding equi-frequency contours for the 27th and 3rd modes, (c-d)

5. ábra Az ω(k) diszperziós összefüggés a 27. és 3. módusra, az első Brillouin zónában lévő összes k vektor szerint, (a-b). Megfelelő ekvi-frekvenciás kontúrok a 27. és 3. módusokhoz, (c-d)

4. Conclusions

The FEM method was applied to investigate the dispersion curves of phononic crystals with quasi-Sierpinski carpet unit cells. Two new quasi-Sierpinski carpets were presented and the results show absolute bandgaps. The influence of the different configurations of the 4th order Sierpinski carpet on the bandgaps was demonstrated. The proposed quasi-Sierpinski carpets can be used to attain larger bandgaps than those observed with traditional Sierpinski carpets. Therefore, the appropriate modifications by retaining self-similarity to some degree and suitable fractal order of Sierpinski carpet structure can be utilized to extend vibration-free zones without changing the entire size of the phononic crystal. Compared to the traditional Sierpinski fractals in a regular configuration, it is also easier to increase the filling fraction to observe the band gap features.

Acknowledgements

One of the authors, Ekmel Ozbay, acknowledges partial support from the Turkish Academy of Sciences.

References

[1] Maier, S. (2018) World Scientific Handbook of Metamaterials and Plasmonics, Vol. 2 Elastic, acoustic and seismic metamaterials. *World Scientific, Singapur*, 658 p. https://doi.org/10.1142/1064

[2] Palaz, S., Ozer, Z., Mamedov, Amirullah M., Ozbay, E. (2020) Ferroelectric based Fractal Phononic Crystals: Wave Propagation and Band Structure. *Ferroelectrics*. 557(1), 85, https://doi.org/10.1080/00150193.2020.1713352

[3] Gouyet, J-F. (1996) Physics and Fractal Structures. *Springer*, *Heidelberg*, 234 p.

[4] Yan, Z., Zhang C., Wang Y. (2013) Elastic Wave Localization in Layered Phononic Crystals with Fractal Superlattices, *J. Vib. Acoust*., 135, 041004, https://doi.org/10.1115/1.4023818

[5] Gao, N., Wu, J. H., Jing, L. (2015) Large bandgaps in two-dimensional phononic crystals with self-similarity structure. *International Journal of Modern Physics B*. 29 (4), 1530017, https://doi.org/10.1142/S0217979215500174

[6] Gao, N., Wu, J. H., Jing, L. (2015) Research on the bandgaps of the two-dimensional Sierpinski fractal phononic crystals. *Physica B*. 29, 1550134, https://doi.org/10.1142/S0217984915501341

[7] Norris, R. C., Hamel, J. S. and Nadeau P. (2008) Phononic band gap crystals with periodic fractal inclusions: Theoretical study using numerical analysis. *J. Appl. Phys*. 103, 104908, https://doi.org/10.1063/1.2931955

[8] Kuo, N. K., Piazza, G. (2011) Fractal phononic crystals in aluminum nitride: An approach to ultra high frequency bandgaps. *Appl. Phys. Lett.* 99, 163501, https://doi.org/10.1063/1.3651760

[9] Kuo, N.K., Piazza, G. (2011) Ultra high frequency air/aluminum nitride fractal phononic crystals. *Proceedings of the IEEE International Frequency Control Symposium and Exposition*. 5977313, https://doi.org/10.1109/FCS.2011.5977313

[10] Liu, X., Fan, Y., An, Y. (2013) The influence of T-square fractal shape holes on the band structure of two-dimensional phononic crystals. *Physica B*. 429, 73–78, https://doi.org/10.1016/j.physb.2013.08.007

[11] Wang, Y. F., Wang, Y. S., Su, X. X., (2011) The influence of T-square fractal shape holes on the band structure of two-dimensional phononic crystals. *J. Appl. Phys*. 110, 113520, https://doi.org/10.1016/j.physb.2013.08.007

[12] Wang, K., Liu, Y., Liang, T. S. (2016) Band structures in sierpinski triangle fractal porous phononic crystals. *Phys. B*. 498, 33–42, https://doi.org/10.1016/j.physb.2016.06.018

[13] Gao, N., Wu, J. H., Jing, L. (2015) Research on the bandgaps of the two-dimensional Sierpinski fractal phononic crystals. *Mod. Phys. Lett. B*. 29 (23), 1550134, https://doi.org/10.1142/S0217984915501341

[14] Canham, L. (2014) Handbook of Porous Silicon. *Springer*, *Heidelberg*, 1017 p. https://doi.org/10.1007/978-3-319-71381-6

Ref.:
Oltulu, Oral – **Ozer**, Zafer – **Mamedov**, Amirullah M. – **Ozbay**, Ekmel: *Band structures of metacompsosite based phononic crystals in quasi-Sierpinski fractals*
Építőanyag – Journal of Silicate Based and Composite Materials, Vol. 74, No. 2 (2022), 57–60. p.
https://doi.org/10.14382/epitoanyag-jsbcm.2022.9

Feasibility of marble powder and calcined bentonite in SCM as partial substitution of cement for sustainable production

Zine El-Abidine LAIDANI ▪ Civil Engineering Research Laboratory (LRGC), University of Laghouat, Algeria
Younes OULDKHAOUA ▪ Building in Environment Laboratory, Faculty of Civil Engineering, University of Sciences and Technology Houari Boumediene, Algiers, Algeria
Mohamed SAHRAOUI ▪ Civil Engineering Research Laboratory (LRGC), University of Laghouat, Algeria
Benchaa BENABED ▪ Civil Engineering Research Laboratory (LRGC), University of Laghouat, Algeria
Érkezett: 2021. 09. 07. ▪ Received: 07. 09. 2021. ▪ https://doi.org/10.14382/epitoanyag-jsbcm.2022.10

Zine El-Abidine LAIDANI
PhD, LRGC Laboratory, University of Laghouat, Algeria. His research interests include self-compacting concrete technology, Calcined clays.

Younes OULDKHAOUA
Assistant professor Faculty of Civil Engineering, USTHB, Algiers, Algeria. His research interests include rheology, mechanical and durability properties of self-compacting concrete.

Mohamed SAHRAOUI
PhD, LRGC Laboratory, University of Laghouat, Algeria. His research interests include self-compacting concrete, Design of experiments and neural network.

Benchaa BENABED
Professor at the Department of Civil Engineering, University of Laghouat, Algeria. His research interests include self-compacting concrete, rheology and durability of concrete.

Abstract
Global cement production has increased dramatically in recent years, and it is now the third largest source of carbon dioxide emissions. The use of binary and ternary cement in production of new binder leads to more debates on the reduction of CO_2 emissions. The main goal of this paper is to investigate the feasibility of marble powder (MP) and calcined bentonite (CB) as partial substitution of cement. In this experimental study, nine mixtures of self-compacting mortar (SCM) were prepared by substituting the cement with MP and CB in ternary blend systems. SCM was tested at fresh state with mini slump flow and mini V-funnel flow time. At hardened state, compressive strength, density, water absorption and ultrasonic pulse velocity (UPV) were measured. The results indicated that the inclusion of MP and CB mixtures improved the flowability of SCM. The use of ternary blended cements based on CB and MP increased the mechanical properties with a content ranging from 15 to 20%. This result has a positive impact on reducing the amount of CO_2 emitted into the atmosphere by combustion cement plants, resulting in a much cleaner environment.
Keywords: self-compacting mortar, calcined bentonite, marble powder, ternary cement
Kulcsszavak: öntömörödő habarcs, kalcinált bentonit, márványpor, háromkomponensű cement

1. Introduction

The cement industry consumes a considerable amount of energy [1] and therefore produces a significant quantity of greenhouse gas [2]. This gas results from the combustion of fuel and the decarbonation of $CaCO_3$, contained in the raw material, during the clinkerization process. Ternary cements are one of the alternative solutions, in which clinker in Portland cement is partially replaced with a combination of two supplementary cementing materials (SCM) in order to preserve or improve the performance of the cement [3]. Limestone Calcined Clay Cement or LC3 is a ternary binder system consisting of limestone and calcined clay used in conjunction to make a composite cement. in these ternary cement systems, a synergetic effect is developed which aluminate from the metakaolin reacts with calcite and enhances the formation of carboaluminate phases [4, 5]. Similarly, marble stone calcined clay cement (MC3) is produced and checked the physical and chemical properties of these cement [6]. LC3 has attracted a great deal of attention within recent years according to the even higher clinker replacement levels and achieve properties comparable to that of the conventional concrete [7]. Ergün [8] reported that the concrete specimens containing 5% of MP and 10% of diatomite as cement replacement had higher compressive strength than that of the control concrete. The results that concrete made using 5% of MP and 10% of Diatomite as cement replacement had highest compressive and flexural strength. Another anterior investigation [9] pointed out that an improvement in the workability of self-compacting concrete (SCC) with the use of natural pozzolan and marble powder, while that the use of 5% MP and 5% of pozzolan, leads to obtain better compressive strength at 28 days. Baoguo et al [10] have noticed that the combination between 10 % of marble powder (MP) and 3% of nano-silica, could partially offset the negative effect caused by each other and obtain acceptable hardened properties of mortars. On the other hand, recent works [11, 12] have allowed to know the usefulness of bentonite clay calcination which offers an excellent pozzolan, considered as judicious solution to minimize the use of cement in concrete.

The main goal of this paper is to investigate experimentally the effect of low carbon cement consists of MP and CB as ternary cement on fresh and hardened properties of SCM for sustainable production.

2. Materials and experimental program

2.1 Materials

For all mortar mixtures, an Ordinary Portland Cement CEM I 42.5 was used. MP is a waste resulting from cutting, shaping and lustrating of the marble stones. CB was obtained by thermal treatment of a local bentonite clay at 800 °C in an electrical furnace for 3 h. The calcination procedure was chosen according to a previous work [12]. The chemical composition and physical properties of raw materials are given in *Table 1*. According to this table, the chemical composition of MP is mainly CaO, which is more than 56%. While Al_2O_3 and SiO_2 are the most dominant compositions in CB (>80%).

The crystalline phases in MP and CB were analyzed by XRD and shown in *Fig. 1*. It shown that MP is mainly composed of calcite with some traces of the quartz and dolomite. For CB, quartz and illite were accompanied with albite, microcline and high temperature crystalline phases such as mullite in addition to slight presence of anatase. *Fig. 2* illustrates the particle size distribution of both of MP and CB compared to cement.

As fine aggregate, a river sand was used with fineness modulus, specific gravity and water absorption of 2.43, 2.68 and 0.79 respectively.

A polycarboxylate superplasticizer (SP) with a specific gravity of 1.07 and a solid content of 30% was used as a high range water reducer in SCC mixtures to achieve the desired flowability.

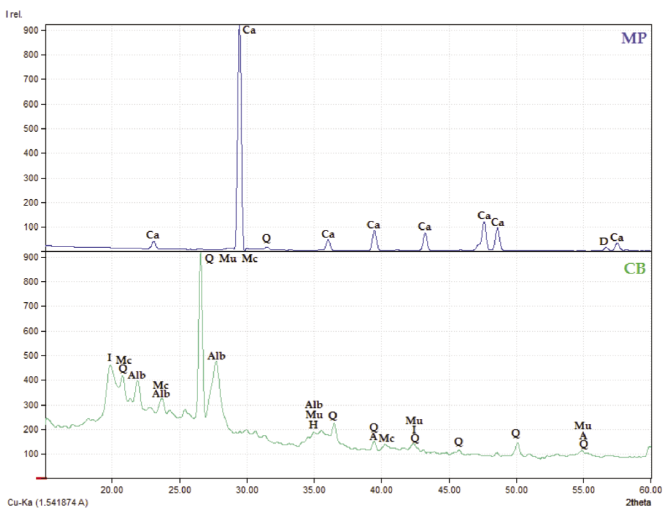

Fig. 1 XRD Analysis of calcined bentonites
(Ca :Calcite, D:Dolomite; Q: quartz; Alb: Albite; Mc: Microcline; Mu: Mullite; I: Illite; H: Hematite; A: Anatase)
1. ábra Kalcinált bentonitok XRD analízise
(Ca: kalcit, D: dolomit; Q: kvarc; Alb: albit; Mc: mikroklin; Mu: mullit; I: illit; H: hematit; A: anatáz)

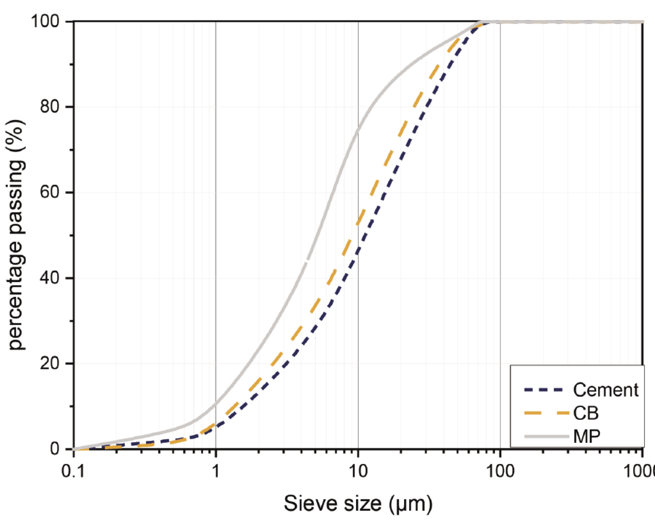

Fig. 2 Particle size distribution of cement, MP and CB
2. ábra A cement, MP és CB szemcseméret eloszlása

Chemical composition	Cement	CB	MP
SiO_2	20.87	63.04	0.51
Al_2O_3	4.17	17.15	0.13
Fe_2O_3	5.65	3.17	0.06
CaO	62.87	1.93	56.24
MgO	1.53	4.12	0.1
K_2O	0.58	1.47	0.01
Na_2O	0.15	2,64	0.45
SO_3	2.29	0.38	0.01
Loss ignition	-	-	42.49
Physical properties			
Specific gravity (g/cm³)	3.08	2.35	2.6
Blaine Fineness (cm²/g)	3344	4371	5243

Table 1 Chemical composition and physical properties of cement, CB and MP
1. táblázat A cement, MP és CB kémiai összetétele és fizikai tulajdonságai

2.2 Mix design

A control mix without any substitution, in addition to eight mix designs with two groups of self-compacting mortar made including MP and CB are performed, in the first group the MP content is fixed at level of 10% by weight of cement, while the CB was replaced in proportions of 5, 10, 15 and 20%. In the second group, the BC content is fixed at the rate of 15% by weight of cement, while the MP was replaced in proportions of 5, 10, 15, and 20%.

The self-compacting formulation criteria proposed by the Japanese Okamura and Ouchi [13] was used for all SCM mixtures, with some modifications regarding the quantity of sand in the mortar (the ratio of sand/mortar (S/M) was fixed at 0.5), the water/binder ratio (W/B) (kept constant at 0.4), the dosage of superplasticizers (SP). The SCM mixtures proportions are shown in *Table 2*.

The mixing procedure consisted of mixing the powder and sand for 15 s in dry condition to homogenize the mixture for half a minute before adding 70% the water needed with a regular flow for 1 min, and then adding the remaining 30% of water containing SP for another 1 min. The mixing procedure continued for 5 min.

2.3 Experimental setup

The filling ability of SCM was evaluated by the mini-slump flow test. The apparatus consists of a mould in the form of a frustum of cone, 60 mm high with diameter of 70 mm at the top and 100mm at the base. The cone was filled with mortar and the lifted to allow the mortar to spread, and then subsequent diameter of the mortar is measured. The spread mortar was visually checked for any segregation or bleeding [14].

The passing ability of SCM was assessed by a V-funnel flow test [13], where funnel is filled with 1.1 liters of mortar. The V-funnel flow time is the time between opening the orifice and the first daylight appearing when looking vertically down though the funnel [14].

The average compressive strength of six specimens of 40×40×160mm at ages of 3, 7, 28, 56 and 90 days was determined. The ultrasonic pulse velocity (UPV) is measured in accordance with NF P18-418 standard [15] . The density of

Mix. ID	W/B	Water (kg/m³)	Binder (kg/m³)	Binder			Sand (kg/m³)	SP (%)
				Cement (kg/m³)	MP (kg/m³)	CB (kg/m³)		
Control	0.4	275	690	690	0	0	1325	0.8
10MP5CB				586.5	69	34.5		0.8
10MP10CB				552	69	69		0.8
10MP15CB				517.5	69	103.5		0.8
10MP20CB				483	69	138		0.8
15CB5MP				552	34.5	103.5		0.8
15CB10MP				517.5	69	103.5		0.8
15CB15MP				483	103.5	103.5		0.9
15CB20MP				448.5	138	103.5		1

Table 2 SCM mixture proportions
2. táblázat Az egyes keverékek összetétele

hardened SCM is determined in accordance with NF P18-435 standard [16]. While, the water absorption test was carried out in accordance with ASTM C642-97 [17].

3. Results and discussion

3.1 Fresh properties

The effect of MP and CB on the fresh properties of mortars is given in *Fig. 3*. As can be seen from this figure, the slump flow diameters of all obtained mixtures are acceptable according to the ranges suggested by Domone and JIN [14]. However, it is noticeable that the slump flow of the first group is affected by the CB content, whereas the flowability of mortars decreased as the CB amount increased. This is caused by the fine particles of CB, which have higher surface areas. This result is consistent with several studies [11, 12, 18], which reported the beneficial influence of MP, ensuring a quantity of water destined to the deflocculation and dispersion of cement in one hand. In the other hand CB particles without the need for an additional quantity of water or SP. Khushnood et al [19] concluded that, higher water and superplasticizer demand are required, when CB is used in the self-compacting system. For the second group it is clearly that increasing the quantity of MP lead to an improvement in workability of mixtures. Belaidi et al [9] attributed this gain in workability to the dilution effect generated by marble powder, which proves its effective role in minimizing SP consumption. Ma et al [10] pointed that MP decreased the water requirement and increased the fluidity of mixtures.

In terms of passing ability through the V-funnel, it is clearly that all the values obtained are inside the targeted domain (2 to 10 s). The results obtained show an increase in flow time as the CB content increases for the first group. Contrary to second group, where the incorporation of MP reduces the viscosity of the mixtures, which translates into low V-funnel flow times. Boukhelkhal et al [20] reported similar results in which for the same SP dosage, the use of MP in SCC lead to a reduction in flow time. Laidani et al [12] indicated that incorporating CB increased the flow time of SCM. Khushnood et al [19] pointed out that the increase in V-funnel flow time and T25 of self-compacting pastes containing bentonite, is probably due to the high friction between particles offered during the flow. Belaidi et al [9] concluded that, at a constant W/B ratio and SP content, the use of both pozzolan and MP by substitution to cement has no negative effects on the workability of SCC.

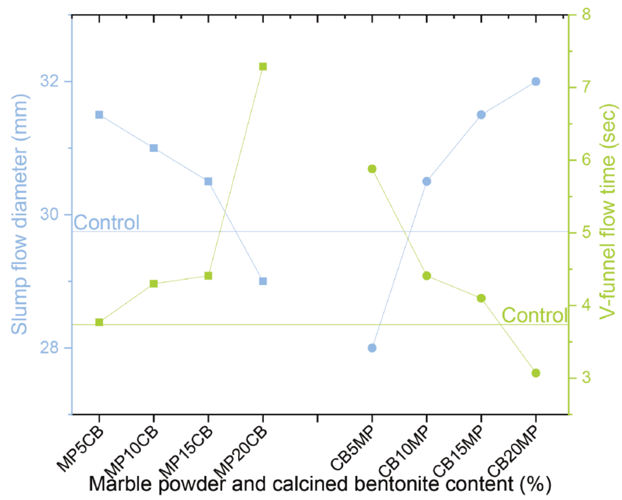

Fig. 3 Slump flow test and V-funnel flow time of SCM made with MP and CB
3. ábra MP és CB alkalmazásával készült cement kiegészítő anyagok roskadásvizsgálati eredményei és V-tölcséres folyási idői

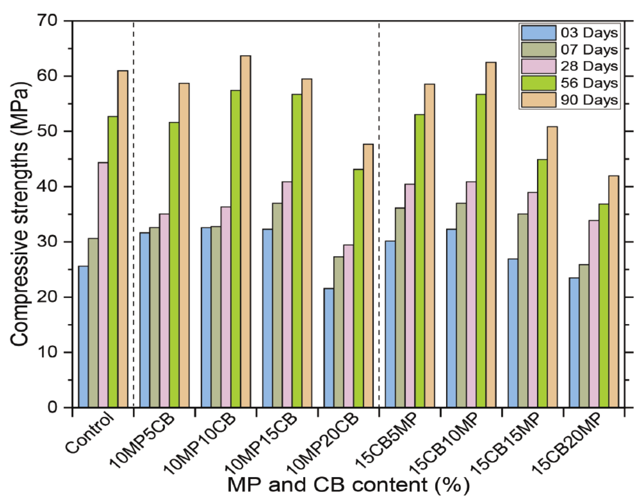

Fig. 4 Compressive strengths of SCM made with MP and CB
4. ábra MP és CB alkalmazásával készült cement kiegészítő anyagok nyomószilárdsági eredményei

3.2 Compressive strength

The compressive strength of all SCM mixes with varying quantities of CB and MP is determined after 3, 7, 28, and 56 and 90 days of water curing and the test results are presented in *Fig. 4*. The figure indicates that the compressive strength increase substantially in the first days of hydration when cement is substituted with MP and CP (3 and 7 days) this is due to the nature of the MP which classified to the family of quasi inert fillers [21]. This filler has a certain physicochemical activity, which contributes to the acceleration of the hydration of C_3S with the component $CaCO_3$ which consequently improves strength at young ages [22].

As the hydration reaction progress (56 and 90), the strength of mortar mixes starts increasing with the presence of CB. The 56 days compressive strength of control mortar increases from 52 MPa to 57 for mortar mixes made with 10% of CB and 10% of MP similar increases to 56 MPa, for mortar mixes made with 15% of CB and 10% of MP. Moreover, the 90days compressive strength of respective mortar mixes increases from 61 MPa to 64 MPa and 63 MPa, which are 5%, and 3.3% higher than the control mix, this is explained by the pozzolanic reaction of CB with $Ca(OH)_2$ and the acceleration of the hydration of OPC [11, 23]. However the combination of two additions reduced slightly the compressive strength when the level of 30% of additions of seems ternary mixes, this phenomenon is due to the effect of the high rate of fine particles which absorb the water necessary for the hydration of the cement which improves the compactness of mixes [24].

3.3 UPV and density

The effects of MP and CB on density and ultrasonic pulse velocity are presented in *Fig. 5* and *Fig. 6* respectively. From these figures it can be generally revealed that the trends in density and UPV are similar to those in compressive strength, which confirm the concurrent development and the strong correlation between density, compressive strength and the sound transmission velocity [20, 25]. It can be also seen that the density and UPV values of the first group increased with the increase of MP proportion until a maximum value (corresponding to the rate of 10% of both MP and CB) and then decreased. This can be attributed to the fact that calcite from MP reacts with aluminate from CB and contribute to the formation of carboaluminate that helps in providing more compactness [4]. Moreover, MP fills the void between cement particles owing to its higher fineness. Once the space between cement particles is completely filled, MP then began to occupy the place of cement particles, and therefore the density and the sound transmission velocity decreases [26-28]. It should be noted that the lower specific gravity of MP also contributes to a decrease in UPV and density of hardened SCM [20, 28].

Test results of the second group indicate that SCM mixtures with 15% of CB and 10% of MP show the maximum density and UPV values. Beyond this optimum, the density and UPV decrease. The synergistic effect of CB and MP accelerate the internal structure development by the formation of additional hydrates, which leads to an increase in density and sound transmission velocity. Furthermore, the total porosity decreases because of to the filling effect of CB inside the skeleton of SCM. Beyond a 15% of CB substitution, there was a reduction in density and UPV and that is due to the fact that CB fine grains began to take the place of cement particles, this led to a reduction in compactness at high amounts of substitutions. Moreover, the higher CB replacements could also absorb the water demand destined for hydration process [12].

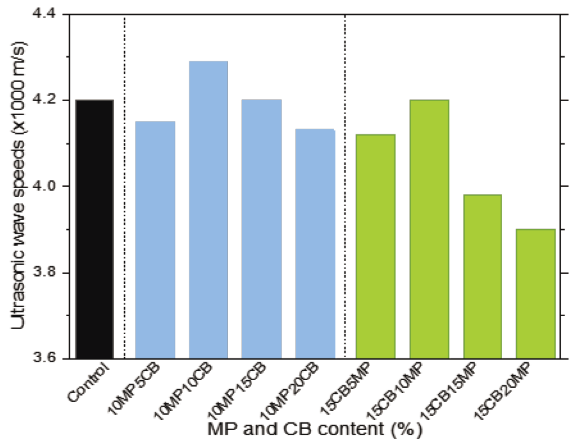

Fig. 5 UPV of SCM made with MP and CB
5. ábra MP és CB alkalmazásával készült cement kiegészítő anyagok ultrahang impulzussebességei

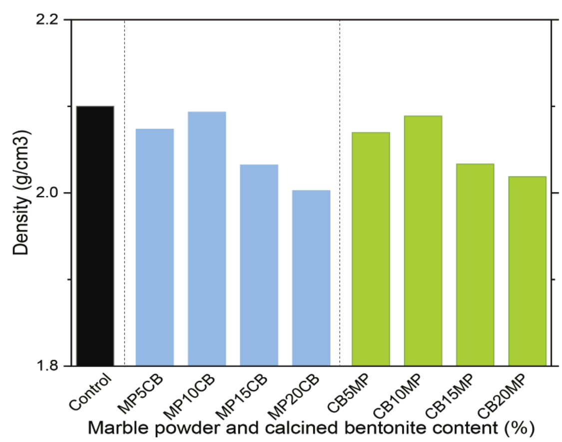

Fig. 6 Density of SCM made with MP and CB
6. ábra MP és CB alkalmazásával készült cement kiegészítő anyagok sűrűségi adatai

3.4 Water absorption

The results of water absorption by total immersion of all mixtures measured at 28 days are illustrated in *Fig. 7*. According to this Figure, its noticeable that the water absorption of both groups are increased by increasing the rate of substitution. In addition, all absorption values are greater than that of control mixture (6.9%).

As optimum, the lowest water absorption value is registered for the mortar 10MP5BC (7.1%), beside that the first group had a lower absorption potential than the second group. This may be due to the filling role of MP, where its grains fill the porous system because they are finer than the cement and CB, in addition to the production of additional C-S-H generated during the pozzolanic reaction between CB and MP. It was noted, that all tested SCM have low water absorption, which is less than 10%.

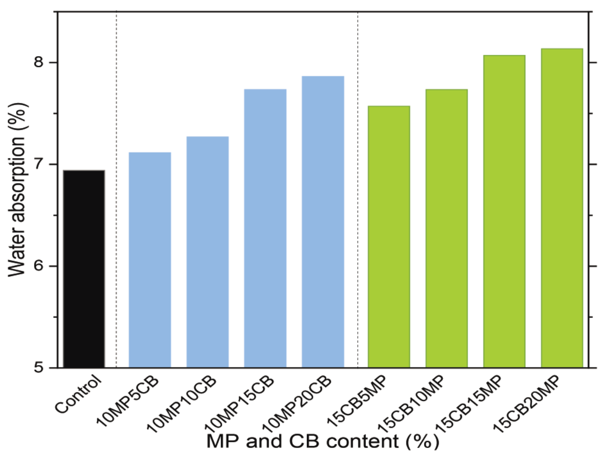

Fig. 7 Water absorption of SCM made with MP and CB
7. ábra MP és CB alkalmazásával készült cement kiegészítő anyagok vízfelvétele

4. Conclusions

Based on the experimental results and the analysis performed, the following conclusions can be drawn:

1. The increase in CB affected negatively the fresh properties and rheological parameters of all mixtures.
2. The use of MP in CB mixtures as ternary cement have shown high fluidity and viscosity of SCM; this increased would have important benefits to improve the fresh quality of SCM production.
3. The compressive strength of all SCM improve with introduction of MP at young age, this increase stabilize beyond 28 days. The substitution of cement with 15% CB as ternary cementitious blends increased the compressive strength of the control SCM mixture by 10% and 5% at 56 and 90 days, respectively.
4. Maximum density and UPV is obtained for mixtures composed of 10% of MP and 10% or 15% of CB, which confirm the presence of synergistic effect between calcined clays and calcium carbonate fillers.
5. The absorption of water increased as the amount of ternary cement (MP+CB) increased.
6. The feasibility use of combination of MP and CB at replacement rate of 15 or 20% to produce a new ternary blended cement in order to reduce the CO_2 emissions for sustainable development.

Acknowledgements

The authors gratefully acknowledge the Directorate-General of Scientific Research and Technological Development of Algeria (DGRSDT) for its valuable support.

References

[1] C.-Y. Zhang, B. Yu, J.-M. Chen, Y.-M. Wei, Green transition pathways for cement industry in China, Resources, Conservation and Recycling 166 (2021) 105355. https://doi.org/10.1016/j.resconrec.2020.105355

[2] S. Gupta, B. Mohapatra, M. Bansal, A review on development of Portland limestone cement: A step towards low carbon economy for Indian cement industry, Current Research in Green and Sustainable Chemistry 3 (2020) 100019. https://doi.org/10.1016/j.crgsc.2020.100019

[3] R.A. Rivera, M.Á. Sanjuán, D.A. Martín, J.L. Costafreda, Performance of Ground Granulated Blast-Furnace Slag and Coal Fly Ash Ternary Portland Cements Exposed to Natural Carbonation, Materials 14(12) (2021) 3239. https://doi.org/10.3390/ma14123239

[4] F. Avet, K. Scrivener, Investigation of the calcined kaolinite content on the hydration of Limestone Calcined Clay Cement (LC3), Cement and Concrete Research 107 (2018) 124-135. https://doi.org/10.1016/j.cemconres.2018.02.016

[5] S. Krishnan, S.K. Kanaujia, S. Mithia, S. Bishnoi, Hydration kinetics and mechanisms of carbonates from stone wastes in ternary blends with calcined clay, Construction and building materials 164 (2018) 265-274. https://doi.org/10.1016/j.conbuildmat.2017.12.240

[6] S. Gunjal, B. Kondraivendhan, Study on Fresh and Harden Properties of Limestone Calcined Clay Cement (LC 3) Production by Marble Stone Powder, Calcined Clays for Sustainable Concrete, Springer2020, pp. 535-543. https://doi.org/10.1007/978-981-15-2806-4_60

[7] H. Du, S. Dai Pang, High-performance concrete incorporating calcined kaolin clay and limestone as cement substitute, Construction and Building Materials 264 (2020) 120152. https://doi.org/10.1016/j.conbuildmat.2020.120152

[8] A. Ergün, Effects of the usage of diatomite and waste marble powder as partial replacement of cement on the mechanical properties of concrete, Construction and building materials 25(2) (2011) 806-812. https://doi.org/10.1016/j.conbuildmat.2010.07.002

[9] A. Belaidi, L. Azzouz, E. Kadri, S. Kenai, Effect of natural pozzolana and marble powder on the properties of self-compacting concrete, Construction and Building Materials 31 (2012) 251-257. https://doi.org/10.1016/j.conbuildmat.2011.12.109

[10] B. Ma, J. Wang, H. Tan, X. Li, L. Cai, Y. Zhou, Z. Chu, Utilization of waste marble powder in cement-based materials by incorporating nano silica, Construction and Building Materials 211 (2019) 139-149. https://doi.org/10.1016/j.conbuildmat.2019.03.248

[11] Z.E.-A. Laidani, B. Benabed, R. Abousnina, M.K. Gueddouda, E.-H. Kadri, Experimental investigation on effects of calcined bentonite on fresh, strength and durability properties of sustainable self-compacting concrete, Construction and Building Materials 230 (2020) 117062. https://doi.org/10.1016/j.conbuildmat.2019.117062

[12] Z.E.-A. Laidani, B. Benabed, R. Abousnina, M.K. Gueddouda, M.J. Khatib, Potential pozzolanicity of Algerian calcined bentonite used as cement replacement: optimisation of calcination temperature and effect on strength of self-compacting mortars, European Journal of Environmental and Civil Engineering (2020) 1-23. https://doi.org/10.1080/19648189.2020.1713898

[13] H. Okamura, M. Ouchi, Self-compacting concrete, Journal of advanced concrete technology 1(1) (2003) 5-15.

[14] P. Domone, J. JIN, Properties of mortar for self-compacting concrete, Self-compacting concrete (Stockholm, 13-14 September 1999), 1999, pp. 109-120.

[15] AFNOR NF P18-418, Béton- Auscultation sonique. Mesure du temps de propagation d'ondes soniques dans le béton, Normalisation française, 1989, p. 1-12.

[16] P 18-435 (2001) Hardened concrete testing - Part 7: Bulk density of concrete.

[17] C. ASTM, 642, Standard test method for density, absorption, and voids in hardened concrete, Annual book of ASTM standards 4 (2006) 02.

[18] S.A. Memon, R. Arsalan, S. Khan, T.Y. Lo, Utilization of Pakistani bentonite as partial replacement of cement in concrete, Construction and Building Materials 30 (2012) 237-242. https://doi.org/10.1016/j.conbuildmat.2011.11.021Get

[19] R.A. Khushnood, S.A. Rizwan, S.A. Memon, J.-M. Tulliani, G.A. Ferro, Experimental investigation on use of wheat straw ash and bentonite in self-compacting cementitious system, Advances in materials science and engineering 2014 (2014). https://doi.org/10.1155/2014/832508

[20] A. Boukhelkhal, L. Azzouz, A.S.E. Belaïdi, B. Benabed, Effects of marble powder as a partial replacement of cement on some engineering properties of self-compacting concrete, Journal of adhesion science and Technology 30(22) (2016) 2405-2419. https://doi.org/10.1080/01694243.2016.1184402

[21] M. Uysal, M. Sumer, Performance of self-compacting concrete containing

different mineral admixtures, Construction and Building materials 25(11) (2011) 4112-4120. https://doi.org/10.1016/j.conbuildmat.2011.04.032

[22] V. Bonavetti, H. Donza, G. Menendez, O. Cabrera, E. Irassar, Limestone filler cement in low w/c concrete: A rational use of energy, Cement and Concrete Research 33(6) (2003) 865-871. https://doi.org/10.1016/S0008-8846(02)01087-6

[23] Y. Ouldkhaoua, B. Benabed, R. Abousnina, E.-H. Kadri, J. Khatib, Effect of using metakaolin as supplementary cementitious material and recycled CRT funnel glass as fine aggregate on the durability of green self-compacting concrete, Construction and Building Materials 235 (2020) 117802. https://doi.org/10.1016/j.conbuildmat.2019.117802

[24] A. Katz, H. Baum, effect of high levels of fines content on concrete properties, ACI Materials Journal 103(6) E (2006) 474.

[25] M. Uysal, K. Yilmaz, Effect of mineral admixtures on properties of self-compacting concrete, Cement and Concrete Composites 33(7) (2011) 771-776. https://doi.org/10.1016/j.cemconcomp.2011.04.005

[26] I.B. Topcu, T. Bilir, T. Uygunoğlu, Effect of waste marble dust content as filler on properties of self-compacting concrete, Construction and building Materials 23(5) (2009) 1947-1953. https://doi.org/10.1016/j.conbuildmat.2008.09.007

[27] M. Belouadah, Z.E.A. Rahmouni, N. Tebbal, Experimental characterization of ordinary concretes obtained by adding construction waste (glass, marble), Procedia Computer Science 158 (2019) 153-162. https://doi.org/10.1016/j.procs.2019.09.038

[28] K.S.A. Kabeer, A.K. Vyas, Utilization of marble powder as fine aggregate in mortar mixes, Construction and Building Materials 165 (2018) 321-332. https://doi.org/10.1016/j.conbuildmat.2018.01.061

Ref.:
Laidani, Zine El-Abidine – **Ouldkhaoua**, Younes – **Sahraoui**, Mohamed – **Benabed**, Benchaa: *Feasibility of marble powder and calcined bentonite in SCM as partial substitution of cement for sustainable production*
Építőanyag – Journal of Silicate Based and Composite Materials, Vol. 74, No. 2 (2022), 61–66. p.
https://doi.org/10.14382/epitoanyag-jsbcm.2022.10

Digital image processing method for evaluation of discoloration on fair-faced concrete surfaces

Kitti AJTAYNÉ KÁROLYFI is assistant lecturer and PhD student at the Department of Structural and Geotechnical Engineering, Széchenyi István University. Area of scientific interest: concrete technology, fair-faced concrete, digital image processing.

Ferenc PAPP is DSc professor at the Department of Structural and Geotechnical Engineering, Széchenyi István University. Area of scientific interest: design and analysis of steel structures, CAD/CAM systems, overall imperfection method.

András HORVÁTH is associate professor at the Department of Physics and Chemistry, Széchenyi István University. Area of scientific interest: digital image processing, simulation of human color perceiption, retina simulation.

K. Ajtayné KÁROLYFI ▪ Department of Structural and Geotechnical Engineering, Széchenyi István University, Hungary ▪ karolyfi.kitti@sze.hu

A. HORVÁTH ▪ Department of Physics and Chemistry, Széchenyi István University, Hungary ▪ horvatha@sze.hu

F. PAPP ▪ Department of Structural and Geotechnical Engineering, Széchenyi István University, Hungary ▪ pappfe@sze.hu

Érkezett: 2021. 09. 07. ▪ Received: 07. 09. 2021. ▪ https://doi.org/10.14382/epitoanyag-jsbcm.2022.11

Abstract

In the case of fair-faced concrete surfaces the architect is responsible for defining the aesthetical requirements, the applicable examination methods and the conformity criterias. The surface quality can be defined by using the national or international standards and guidelines or by setting up specific evaluation aspects and methods. However, regarding the variety of these surfaces, the assessment can be very subjective in some cases and depends on the culture of the given country, especially when considering the discoloration. This paper presents an evaluation method for discoloration of the fair-faced concrete surfaces using digital image processing techniques. The program was written in Python, as a part of a more extensive project including further evaluation aspects of these surfaces. The method was tested on 24 concrete surfaces. Results show, that the changes in concrete composition or in the dimensions of the sample can be observed in the colour tone of the surface, however the automatic method should be supported by subjective evaluation to get the right classification.

Keywords: fair-faced concrete, surface quality, discoloration, digital image processing

Kulcsszavak: látszóbeton, felületi minőség, színeltérés, digitális képfeldolgozás

1. Introduction

The evaluation of fair-faced concrete surfaces is mainly subjective according to the current regulation, especially in the case of colour uniformity. The European standards and guidelines generally determine four surface classes based on different evaluation criterias. In Hungary, there is no dedicated standard for fair-faced concrete surfaces, the MSZ EN 24803-6:3 Specifications for appearance of concrete and reinforced concrete structures [1] can be used for the evaluation. The criterias of the standard are categorized in two groups: the local surface conditions and shape conformity. The latter contains specifications for deterioration of surface quality, which can be assessed by comparing the surface to the previously accepted reference surface. The German Code of Practice on Fair-Faced Concrete [2] was published in 2004. It defines four concrete classes with more differentiated subclasses, although it does not provide evaluation methods compared to the Hungarian standard. The criterion of discoloration has three levels (FT1-FT3), in which the staining due to rust or contamination is not allowed. The light or dark discoloration is permitted in the case of the lowest class (FT1), while in the case of FT3 only to a small extent. The classification of the Austrian ÖNORM B 2211 [3] standard is less structured, the aspect of discoloration has only two subclasses. Based on the standard, the Guideline of Formed Concrete Surfaces [4] clarifies the evaluation criterias and introduces new aspects as well. The discoloration is evaluated subjectively by using a grey colour chart (*Fig. 1.)*: the guideline defines the maximal number of the present neighbouring colours for the three subclasses. In the case of the lowest class (FT1) the presence of 5 consecutive colour tones is allowed, and 3 for the highest class (FT3).

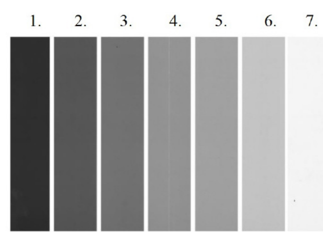

Fig. 1 Grey colour chart according to the Austrian guideline
1. ábra Az osztrák irányelv szerinti szürkeszín skála

The research of colour uniformity of fair-faced concrete surfaces is mainly focusing on the root causes of this phenomenon to facilitate its practical application. These research materials [5, 6, 7, 8, 9, 10, 11] are providing detailed information about the effect of the different factors on the colour uniformity of the surface such as the applied formwork material, the concrete composition, the release agent, the construction process or the environmental conditions. Based on the results, authors are developing useful proposals for the practice. The applied evaluation method depends on the type of the research material: the practical guidelines and summarizing literatures are using visual inspection [5, 6, 7, 8], while the scientific materials [9, 10, 11] are using professional tools, such as light microscopy, scanning electron microscopy, infrared spectrophotometry or dispersive X-Ray analysis. However, the visual inspection is mainly subjective, while the latter tools are only applicable in laboratory environment. Only a few research materials [12, 13] are available in the topic of developing objective evaluation method that can be used on site as well. This paper presents a new assessment method for colour uniformity of fair-faced concrete surfaces based on digital image processing and using grey colour chart of the Austrian guideline.

2. Research method

For the investigations 12 fair-faced concrete samples were made (*Fig.2.*) by using 3 moulds of different sizes and 4 types of concrete mixtures presented in the authors' former paper [14]. The formwork was made from layered plywood with melamine resin coating, and the applied sizes were the followings: 10×50×50 (F-1), 20×50×50 (F-2) and 30×50×50 (F-3) cm. The four concrete compositions contained increasing amount of cement and water and decreasing amount of aggregate, which resulted in varying content of cement paste beside a constant water-to-cement ratio (v/c = 0.50). The first mixture was slightly oversatured with an excess of 76 l/m^3 (1) cement paste beyond the cement paste demand of the aggreagate. After that, the saturation degree was increased for 101 (2), 126 (3) and 150 l/m^3 (4). The concrete was filled in 3 layers and it was compacted by using an internal vibrator in a net of 5 cm for 5 seconds in every point. The samples were kept in moulds for 3 days.

Fig. 2. A part of the samples
2. ábra Az elkészített próbatestek egy része

Digital image processing method was used for the evaluation of the surfaces. Two images were made of both sides of the samples from equal distance (70 cm) by using a digital camera of the type SONY DSC-HX350. The images were made under the same lighting conditions at the same time using only the flash of the camera. Before the photography a scaling marker and two certificated grey colour chart was attached to the samples according to the Austrian guideline, which is the basis of the evaluation of discoloration (*Fig. 3.)*. The exact colour of the different grey tones was determined on the greyscale images by using the GIMP software by averaging the values of the same tone on the upper and bottom colour chart. Based on the values of the 7 tones 8 intervals were determined for the evaluation: (1) darker pixels than the 1. colour tone, (2)-(7) pixels between the neighbouring colour tones, (8) lighter than the 7. colour tone.

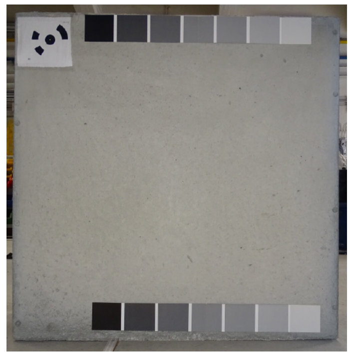

Fig. 3. Image made of the F-3-1 sample
3. ábra az F-3-1 próbatestről készített fénykép

The program was written in Python 2.7 as a development of an existing program made by the authors [15], which can be applied primarily for the automatic evaluation of surface void ratio. The input data is the average value of the 7 colour tones and the greyscale image. The first step is to define the real size of the image and to calculate the factors of the pixel-mm conversion with the help of the marker. After that, a reference surface is cut out from the original image with a size of 50x50 cm. The noise reduction is made by using a Gaussian blur with a kernel of 25x25 pixels, which was already a part of the original program. After this step, the program can read the previously determined grey tone values from an Excel file and defines the number of pixels of the given intervals. As a result, the areas of different colour intervals can be expressed as a percentage of the total surface area. With this small step the program is able to evaluate two main aspects of fair-faced concrete surfaces which are usually difficult to measure.

3. Results

The results can be seen on *Fig. 4-6* depending on the applied formwork size. The surfaces are signed in the following way: Formwork size (F-1-F-3) – Saturation degree of cement paste (1-4) – Site of the sample (1-2). It can be observed, that the dominant grey colour interval was between the second and fourth colour tones on the examined surfaces. In the case of the third and fourth concrete composition, the distribution of the colour intervals is shifted to the right side, which means that the increasing saturation degree of cement paste resulted in lighter surface colour. Furthermore, the covered colour intervals become narrower due to the increase in the formwork size and to the change in concrete composition as well.

These trends can be seen in the curtosis and skewness values of the distributions as well (*Fig. 7*). Skewness is a measure of symmetry of a distribution, while kurtosis is a measure of the tailedness of a distribution relative to a normal distribution. If the skewness is positive, the distribution is shifted to the left side, while in case of a positive kurtosis the distribution has a higher peak than a normal distribution. Here, the graphs are asymmetric, which means that they are skewed to the right and have a peak around the second and third colour intervals, therefore both values are positive in all cases. Furthermore, the skewness and curtosis values become higher with increasing formwork size as well as with increasing saturation degree of cement paste.

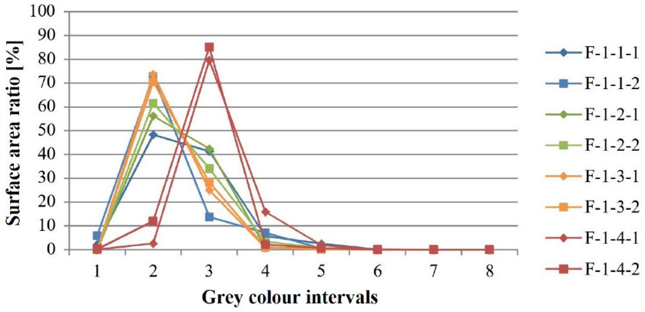

Fig. 4 The surface area ratio of the grey colour intervals in the case of the F-1 formwork
4. ábra Szürkeszín intervallumok aránya a vizsgált felületeken az F-1 zsaluzat esetében

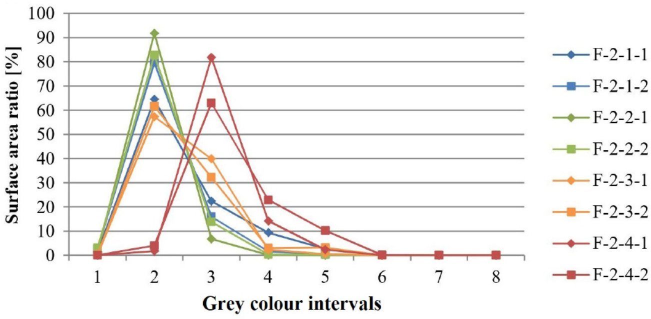

Fig. 5 The surface area ratio of the grey colour intervals in the case of the F-2 formwork
5. ábra Szürkeszín intervallumok aránya a vizsgált felületeken az F-2 zsaluzat esetében

The observations are similar based on the subjective evaluation according to the German and Austrian guidelines. The increasing saturation degree results in more homogenous colour tone of the surfaces, while the increase of the formwork size has also a positive, but reduced effect on surface quality. It means that all of the samples made with the fourth concrete composition have reached the highest class according to the guidelines. Besides that, the samples made by the F-3 formwork have generally the highest surface quality. The classification was also made based on the automatic evaluation method. Here, those colour tones were taken into account, which have reached at least 2% or 5% of the surface area (*Table 1.*). Based on the results, there are 4 samples, whose classification is different from the subjective evaluation if the threshold of 2% was applied, and 5 samples, if the threshold of 5% was used.

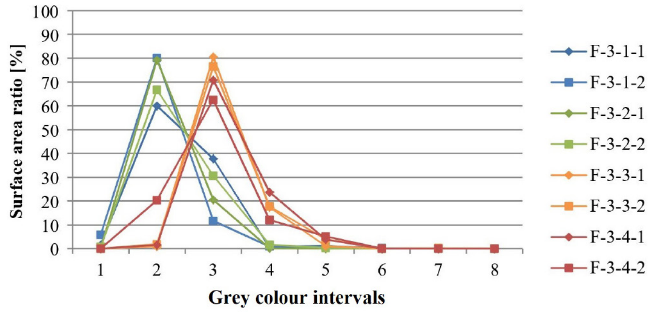

Fig. 6 The surface area ratio of the grey colour intervals in the case of the F-3 formwork
6. ábra Szürkeszín intervallumok aránya a vizsgált felületeken az F-3 zsaluzat esetében

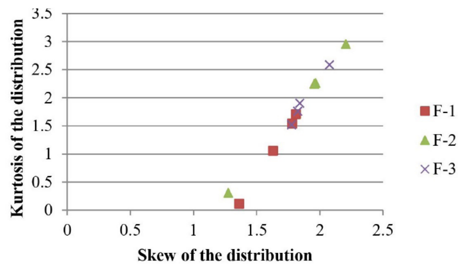

Fig. 7 Correspondences between the skew and kurtosis of the distributions
7. ábra Az eloszlásfüggvények ferdeségi és csúcsossági együtthatóinak összefüggése

4. Conclusions

In this study, a quantitative aspect was introduced into the assessment of discoloration of fair-faced concrete surfaces with the help of digital image processing techniques. It can be

Sample	Class according to the German guideline – subjective evaluation	Class according to the Austrian guideline – subjective evaluation	Class according to the Austrian guideline – automatic evaluation (2%)	Class according to the Austrian guideline – automatic evaluation (5%)
F-1-1	FT1	FT1	FT1	FT1
F-1-2	FT2	FT2	FT2	FT3
F-1-3	FT3	FT3	FT3	FT3
F-1-4	FT3	FT3	FT2	FT3
F-2-1	FT1	FT2	FT1	FT2
F-2-2	FT3	FT2	FT3	FT3
F-2-3	FT1	FT2	FT1	FT3
F-2-4	FT3	FT3	FT1	FT2
F-3-1	FT3	FT3	FT3	FT2
F-3-2	FT3	FT2	FT3	FT3
F-3-3	FT3	FT3	FT2	FT3
F-3-4	FT3	FT3	FT2	FT2

Table 1 Classification of the samples according to the applied guidelines and the proposed method
1. táblázat A felületek osztályba sorolása az alkalmazott irányelvek és a kidolgozott eljárás szerint

concluded, that the effect of a change in concrete composition or formwork size can clearly be observed with the help of the grey colour intervals' distribution. However, the classification made by the automatic evaluation method has different results from the subjective assessment in some cases, which draws attention to the importance of visual inspection. Therefore, the recommended evaluation method can be a useful tool for examination of the effect of different factors (concrete composition, applied materials, formwork sizes and materials, environmental conditions, etc.) on the colour uniformity of the surface, while in the case of classification it is recommended to combine it with subjective evaluation. The proposed method can be further developed to take into account not only the surface area of the different colour tones but also the position and extent of the strains, therefore a more nuanced evaluation of the discoloration would be possible. The developed program can also be extended to further evaluation aspects, such as the arrangement and formation of the formwork ties, the grid system of the joints or the forming of the edges. The digital image processing methods, as the applied Python and its OpenCV module, have several tools for detection of surface irregularities, which can lead to develop an effective and objective evaluation method for fair-faced concrete surfaces.

Acknowledgements

Supported by the ÚNKP-20-4-I-SZE-38 New National Excellence Program of the Ministry for Innovation and Technology from the source of the National Research, Development and Innovation Fund.

References

[1] MSZ EN 24803-6-3:2010 (2010) Épületszerkezetek megjelenési módjának előírásai, Monolit beton- és vasbeton szerkezetek. A helyi alakhűség és a felületi állapot követelményei, Magyar Szabványügyi Testület

[2] Deutscher Beton- und Bautechnik Verein e.V, Bundesverband der Deutschen Zementindustrie (2004) Merkblatt Sichtbeton, 52 p.

[3] *ÖNORM B2211 (1998) Beton-, Stahlbeton- und Spannbetonarbeiten – Werkvertragsnorm, 9 p.*

[4] Österreichischen Vereinigung für Beton- und Bautechnik (ÖVBB) Richtlinie (2002) Sichtbeton – Geschalte Betonflächen

[5] Heiß S. (2011) Farbunterschiede bei Sichtbetonflächen – Ursachen und Vermeidung, Betonfertigteile, BWI – BetonWerk International, Vol. 5. pp. 180-183.

[6] Fiala H., Raddatz J. (2003) Braune Verfärbungen auf Sichtbetonflächen, Beton-Informationen, Vol. 2. pp. 27-33.

[7] Schulz J. Sichtbeton-Mängel - Gutachterliche Einstufung, Mängelbeseitigung, Betoninstandsetzung und Betonkosmetik (2011), Vieweg+Teubner Verlag, Springer Fachmedien Wiesbaden GmbH, 233 p. ISBN 978-3-8348-1401-2

[8] Schulz J. Sichtbeton – Planung – Kommentar Zur DIN 18 217 Betonflächen und Schalungshaut, Friedr. Vieweg & Sohn Verlag, GWV Fachverlage GmbH, Wiesbaden (2006) p. 202. ISBN 978-3-8348-1828-7

[9] Strehlein D. E. Fleckige Dunkelverfärbungen an Sichtbetonoberflächen (2012), Dissertation, Technischen Universität München, 151 p.

[10] Schubert U. Betonwerksteine und Betonpflastersteine – Verfärbungen – Ursachen – Analyse – Behebung, Presentation, (2004), Zentralverband Deutsches Baugewerbe, 32. Fachseminar

[11] Schubert K. Schäufele I. (2011) Neue Sichtbetontechnik – Integration der Erkentnisse zu Wechselwirkungen zwischen Schalungshaut, Trennmittel und Betonoberfläche in die Prozesskette beim Sichtbeton, Schlussbericht der Forschungsstelle(n) Nr. 2, Hochschule Karlsruhe, Technik und Wirtschaft Institut für Angewandte Foschung, AiF-Forschungsvereinigung, Deutscher Beton- und Bautechnik Verein e.V., Karlsruhe, 174 p.

[12] Stanke G. Schlussbericht zum Verbundprojekt Baustellenphotogrammetrie - Photogrammetrisches Verfahren als objektorientiertes Ingenieursystem zur Produktionssicherung in der Bauwirtschaft - Teilvorhaben: Sichtbetonalayse (2003), TU Dresden, Rollei Fototechnik, Dywidag, Gesellschaft zur Förderung angewandter Informatik e.V. (GFaI), Berlin, 36 p.

[13] Gesellschaft zur Förderung angewandter Informatik e.V. (GFaI), Bundesministerium für Wirtschaft und Technologie: Schlussbericht Sichtbeton II./15940 B - Bildgeschützte Bewertungsverfahren für Sichtbetonoberflächen (2003), 42 p.

[14] Ajtayné K. K, Papp F. (2021) Laboratory study of the effect of saturation degree on quality of fair-faced concrete surfaces, Építőanyag – Journal of Silicate Based and Composite Materials, Vol. 73, No. 3, pp. 115–118. https://doi.org/10.14382/epitoanyag-jsbcm.2021.17

[15] Ajtayné K. K., Horváth A., Papp F. (2020) A new assessment methodology for fair-faced concrete surfaces based on digital image processing, Proceedings of the 13th International PhD Symposium in Civil Engineering, Paris, France, pp. 288-295. ISBN: 978-2-9406-4306-6

Ref.:
Ajtayné Károlyfi, K. – **Horváth**, A. – **Papp**, F.: *Digital image processing method for evaluation of discoloration on fair-faced concrete surfaces*
Építőanyag – Journal of Silicate Based and Composite Materials, Vol. 74, No. 2 (2022), 67–70. p.
https://doi.org/10.14382/epitoanyag-jsbcm.2022.11

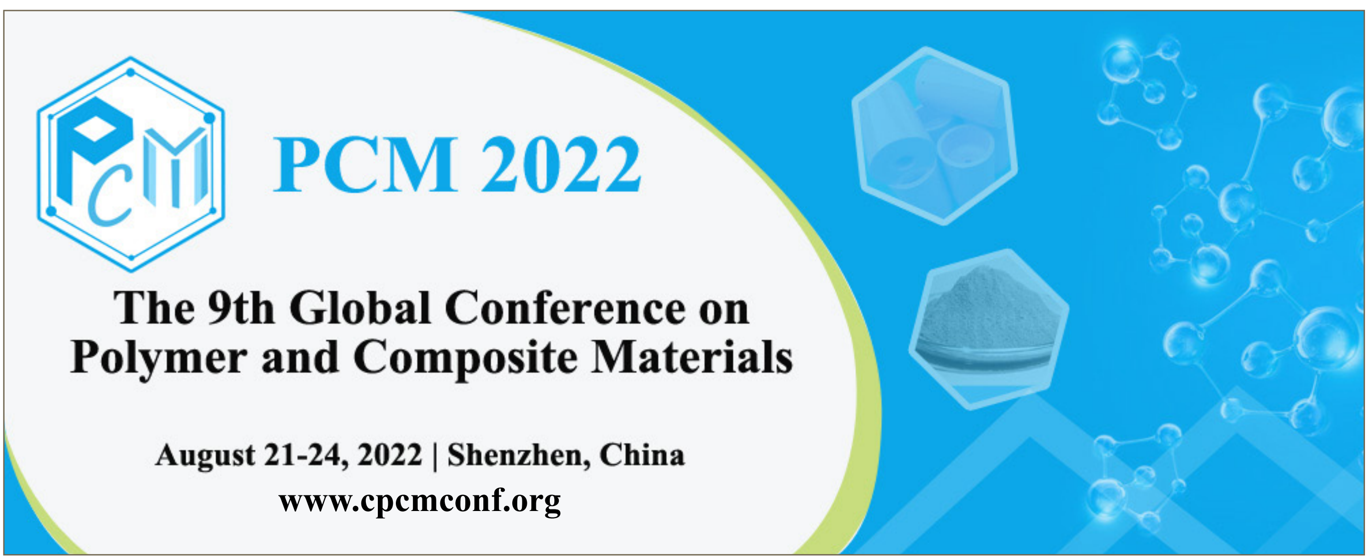

Study of the physicochemical and mechanical compatibility of expanded cork with a cement matrix based on limestone sand

Ahmed ZIREGUE ▪ Civil engineering research laboratory, Amar Thelidji University, Algeria
Benharzallah KROBBA ▪ Civil engineering research laboratory, Amar Thelidji University, Algeria
M.Mouldi KHENFER ▪ Civil engineering research laboratory, Amar Thelidji University, Algeria
Rose-Marie DHEILLY ▪ Reasearch Unit EPROAD, University of Picardie Jules Vernes, France
Justin HOUESSOU ▪ Reasearch Unit EPROAD, University of Picardie Jules Vernes, France
Michèle QUÉNEUDEC-T'KINT ▪ Reasearch Unit EPROAD, University of Picardie Jules Vernes, France
Érkezett: 2021. 09. 07. ▪ Received: 07. 09. 2021. ▪ https://doi.org/10.14382/epitoanyag-jsbcm.2022.12

Abstract

The objective of this work is to study the compatibility of expanded cork with a cement matrix based on limestone sand. This involves analyzing the effect of cork on the microstructure of the produced concrete and on its physicochemical characteristics. Moreover, the elastic compatibility between the cork aggregates with the matrix is studied by comparing the concretes lightened by the cork aggregates with the control concrete. The results obtained show that structurally the cork aggregates have perfect adhesion with the matrix. The incorporation of cork aggregates does not affect the hydration except for a high volume dosage above 70%. The mechanical behavior of the concrete produced shows a considerable difference in compressive strengths and elastic modulus between the control concrete and the lightweight concrete.
Keywords: cork aggregates, microstructure, spectroscopy, compressive strength, modulus of elasticity, compatibility
Kulcsszavak: parafa aggregátumok, mikrostruktúra, spektroszkópia, nyomószilárdság, rugalmassági modulus, kompatibilitás

Ahmed ZIREGUE
Research interests: Lighweigh concrete, insulating materials, Construction Materials, Concrete Durability, Civil Engineering Materials, Composite materials, Recycled materials.

Benharzallah KROBBA
Research interests: Construction Materials, Concrete Durability Concrete Repair, Civil Engineering Materials, Reinforced Concrete, Composite materials, Recycled materials, Self compacting repair materials.

Mohamed Mouldi KHENFER
Research interests: Civil engineering and habitat sciences development of innovative building material with environmental impact and energy efficiency Environment and use of raw materials.

Rose-Marie DHEILLY
Research interests: Engineering of multi-materials: optimization of processes and functionalization of formulations. Application the provision of alternatives to the use of fossil products, the recovery of ordinary industrial waste and the the non-food development of agro-resources.

Justin HOUESSOU
Research interests: The agropolymers materials, Life and Environmental Sciences and Industries, waste valorization, Biobased materials, Analytical Chemistry.

Michèle QUÉNEUDEC-T'KINT
Research interests: Innovant agromaterials, Materials eco-engineering, Agro-sourced thermal insulation, Cement and concrete composites, Lightweight concrete.

1. Introduction

With the development of new design and construction technologies, it's time for the light-weight structures housing. This is why, for several years, concretes based on lightweight aggregates have experienced a real increase in interest throughout the world. In addition to their lightness, they have quite interesting performances [1]. Several studies have been carried out for the elaboration and development of these materials [2–6]. Lightweight aggregates are used in concrete, mortars and screeds to replace conventional mineral aggregates, in order to reduce their weight and improve their thermal and acoustic performance [7–10]. Among these, we must particularly mention lignocellulosic waste which constitutes a major environmental problem because of its abundance. Using this waste as raw material substituted for mineral aggregates could reduce the scale of the problem. [11.12]. This is why the use of renewable lignocellulosic resources, resulting from agriculture or agro-forestry for the development of construction materials has experienced an undeniable resurgence of renewed interest since the end of the 20th century [13]. They are used either as fibers for the reinforcement of building materials, this is the case of hemp, straw, etc, or as aggregates for the manufacture of lightweight insulating concrete to ensure the thermal comfort of the premises. We can cite by way of example wood, cork, etc. Cork is a raw material obtained from the bark of the oak, Quercus Suber, which grows mainly in the Mediterranean basin, especially in the southern regions of the Iberian Peninsula. Portugal is still the world's main producer of cork. The cork is a low density material and provides excellent thermal and acoustic insulation. It is a renewable material, the harvest of which preserves the tree by improving its health and prolonging its lifespan. Cork has low stiffness, low strength and high compressive stresses [1, 14-16]. The oak bark tissue of Quercus Suber used for the production of cork consists of microcells, the shape of which resembles a hexagonal structure connected by capillaries. The interior of these polyhedral is filled with a gas characterized by properties similar to those of air. The solid constituents of cork are approximately 45% lignins - 27% cellulose and polysaccharides - 12% tannin - 6% wax - 5% other substances - 5% [17,18].

Some studies have already been published on materials containing cork granules with cement or gypsum as a binder [1, 14, 19]. The authors presented an experimental study on the use of expanded cork granules with cement-based mixtures to produce lightweight concretes for screeds. The results obtained show that the compressive strength of these materials varies from 0.2 to 2.23 MPa; depending on the cork content and thermal conductivity between 0.194 and 0.318 W m^{-1} K^{-1}. Moreira et al [19] developed a lightweight concrete screed, based on cork aggregates incorporated into a cement matrix, composed of cement and alluvial sand. For this purpose, two-particle sizes of expanded cork were used 3-5 mm and 5-10 mm. Three dosages of cement are used 150, 250 and 400 kg/m^3. In this study, 80% of the volume of sand is replaced by 3-5 mm and 5-10 cork aggregates in equal volume proportions. The results obtained show a reduction in density of more than 50% relative to that of the control concrete. The maximum value of the compressive strength is 2.23 MPa for the maximum cement dosage of 400 kg/m^3, while that of the control concrete is 18.36 MPa. The incorporation of cork aggregates made it possible to lower thermal conductivity by 71%. It can, therefore, be seen that the incorporation of lignocellulosic materials, in particular cork in cement matrices, provides very interesting thermal performance. However, these by-products are not completely compatible with cement matrices, because of the cellulose present in their composition and their very complex physical.and chemical structure. The various soluble organic compounds, such as carbohydrates, glycosides and phenolic compounds, present in cork lead to significant dimensional variations and low mechanical strengths. In addition, the plant material inhibits the setting of cement due to the release of sugars, carboxylic acids and other phytochemicals [20, 21]. On the other hand, lime-based binders are more compatible with bio-sourced aggregates or plant material due to the formation of "secondary" hydration products instead of primary hydration. For cementitious binders, several researchers believe that organic extracts are drawn from the cement solution where they form complexes with the metal ions present. This decreases the concentration of Ca2$^+$ ions in the solution and eventually disrupts the equilibrium of the solution which delays the onset of nucleation of Ca $(OH)_2$ and Calcium Silicate Hydrate (C - S - H) gel. Cork contains less hemicellulosic wood. Furthermore; the main chemical component of cork is "suberine" which is a polymeric compound of long-chain aliphatic alcohols and fatty acids that make cork relatively impermeable [22]. These two aspects should be beneficial from the point of view of cork-cement compatibility [23]. It has also been shown that Mortars with the addition of cork granules are much more stable and less subject to temperature changes, so they are considered more durable [17]. According to several authors, the compatibility of lignocellulosic particles with cementitious matrices can be evaluated according to three criteria, namely: the rate of the heat of hydration, and the delay in the setting of the cement; compressive strength and obviously the aggregate bonding matrix established by the microstructure elaborated concretes [11, 12, 23, 24]. According to Karad et al [25] these three criteria depend closely on the nature of the particles, their size, their density and obviously their dosage. In fact, in his study, Karade showed that the smaller the aggregates, the more they have a negative effect on the hydration of the cement and therefore less compatible. On the other hand, he notices that the more the dosage of cork aggregates increases, the more the compatibility decreases [25].

2. Materials and experimentation

2.1 The raw materials used and their characteristics

The materials used in this study are: calcareous sand 0/3 from crushingwaste,thecompoundcementCPJ-CEMII/B42.5RNA442 and cork aggregates of particle size class 3/8 from cork board industry. The physical characteristics of sand and cork aggregates are presented in *Table 1*. The granulometry of cork forms continuity with that of limestone sand (*Fig. 1*).

	Apparent density (kg/m^3)	Absolute density (kg/m^3)	Sand equivalent (%)	Water absorption (%)	Fineness modulus	Porosity %
calcareous sand	1530	2670	83.1	7.780	2.66	43
cork granules	71	155	/	2.30	/	51

Table 1 Physical characteristics of calcareous sand and cork granules
1. táblázat Mészhomok és parafa granulátum fizikai jellemzői

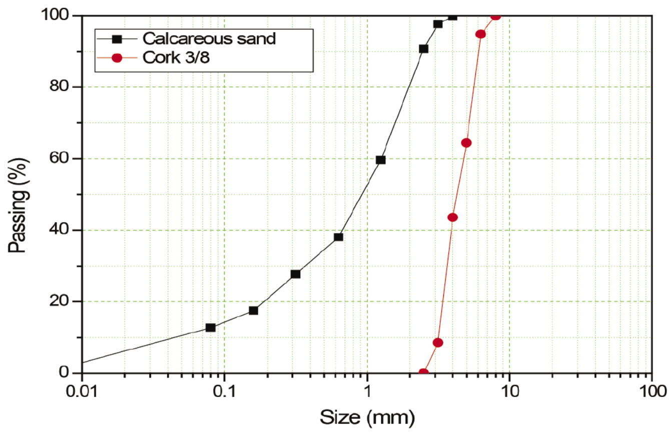

Fig. 1 Particle size distribution of sand and cork
1. ábra Homok és parafa szemcseméret-eloszlása

2.1.1 Cork macrostructure and microstructure

A microscopic view of a cork aggregate (*Fig. 2*) gives an idea of the condition of its exterior surface. It clearly shows a rough condition with openings. This state can promote good adhesion between the cork grain and the matrix. An electron microscope view allows to seeing according to [14] the honeycomb structure of the cork (*Fig. 3*).

Fig. 2 Microscope view of cork granulate 3/8. 40X
2. ábra Parafagranulátum mikroszkóp alatt (3/8. 40X)

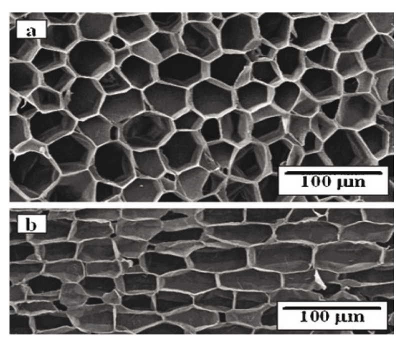

Fig. 3 Cellular structure of cork in the two planes a radial, b tangential [14]
3. ábra A parafa sejtszerkezete két síkban metszve: a) radiális, b) érintőleges [14]

2.1.2 Mechanical characterization of cork

The mechanical tests carried out on the cork show an important elasticity of the cork, in particular in compression. The deformations are very important reaching 90% and the values of the flexural and compressive strengths reach respectively 0.15 MPa and 3.61 MPa respectively. The young's modulus are of the order of 0.92 and 0.66 MPa in flexion and compression, respectively. We can notice that Young's modulus in bending is clearly higher than that observed in compression; this can be explained by the great elasticity of the cork and the very high deformation rate in compression [14, 25, 26].

2.2 Formulation and implementation of concrete

In order to see the influence of the aggregates dosage on the physicomechanical characteristics of the concrete produced, a series of samples was carried out starting with a control concrete corresponding to a zero dosage of aggregates Then, six series of samples corresponding respectively to the volume dosages (aggregates / matrix) of 20%, 30%, 40%, 50%, 60%, 70%. It should be noted that the method of substituting the aggregates used in the series consists in replacing one volume of the matrix (cement + sand + water) by the same volume of aggregates. This allows us to always have a constant cement / sand dosage. The cement dosage used is such that C/S=1/3. The water content was determined from optimization tests on the control mortar and is equal to E/C = 0.6 [18]. In order to compensate for the drop in workability caused by a high dosage of aggregate, a super plasticizer SP40 is used with increasing dosage of 0.5% for the lowest dosage of aggregates to 3% for the maximum dosage. It should be noted that the cork aggregates are pre-wetted 48 hours in water beforehand in order to avoid the absorption of part of the mixing water by the cork aggregates. Then, they are drained on a sieve or absorbent fabric for 4 minutes. The material compositions for the different mixtures are presented in *Table 2*.

We will note CLCC x: Cork Lightweight Calcareous Concrete by x%, x takes the values of 0; 20; 30; 40; 50; 60; 70

Series	A/M (%)	Aggregates mass (kg/m^3)	Sand (kg/m^3)	Cement (kg/m^3)	Needful water (dm^3/m^3)	Super plasticizer (kg/m^3)
CLCC 0	0	0	1380	460	276	0
CLCC 20	20	29.30	1098.4	366.12	219.67	1.83
CLCC 30	30	43.95	961.07	320.35	192.21	3.20
CLCC 40	40	58.60	823.77	274.60	164.75	4.12
CLCC 50	50	73.25	686.48	228.82	137.29	4.58
CLCC 60	60	87.90	549.18	183.06	109.83	4.58
CLCC 70	70	102.55	411.89	137.29	82.38	4.12

CLCC : Cork lightweight calcareous concrete,
A/M : Volume ratio Aggregate / Matrix

Table 2 Weight Composition for the developed concrete materials
2. táblázat A keverékek összetétele

3. Results and discussion

3.1 Structural compatibility

3.1.1 Macrostructural Analysis

Observation of sample sections before crushing showed a more or less good distribution of the aggregates in the matrix (*Fig. 4a*). It is all the better as the dosages are high in aggregates, this is due to the adopted mixing technique. In order to see the matrix-cork aggregate bond well, sample sections were viewed using a Zeiss 80X microscope with 40X magnification (*Fig. 4b*). It can be seen that the aggregate-matrix bond is quite good.

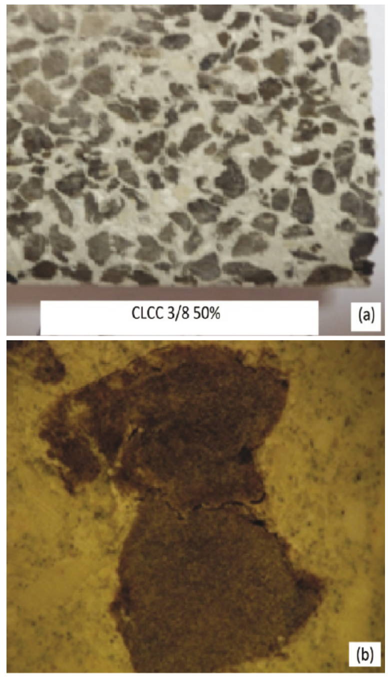

Fig. 4 Concrete's macrostructure
4. ábra A beton makrostruktrája

3.1.2 Microstructural Analysis

Microstructural Analysis, using a scanning electron microscope carried out on two compositions which are the reference concrete CLCC 0 and cork concrete lightened by 50% (CLCC 50%). The results carried out are illustrated in (*Fig 5* and *6*).

3.1.2.1 For the CLCC0

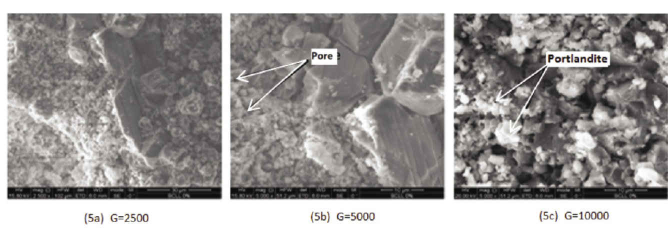

Fig. 5 Micrograph of CLCC0
5. ábra A CLCC0 mikroszkóp alatt

In terms of the general appearance, a good compactness is seen of the cement matrix (*Fig. 5a*). We can see on the *Fig 5b* the existence of pores with a very dark color probably due to the inclusion of air during mixing, or when filling the test tubes. Good adhesion of the sand aggregates with the cement paste is observed in *Fig. 5a* and *Fig. 5b*. A significant presence of orthorhombic dolomite is also observed on *Fig. 5a*. At high magnification (*Fig. 5c*), we were able to identify the nature of the hydration products. Namely mainly C-S-H gels in the form of cotton flowers and Portlandite $Ca(OH)_2$ generally encountered in cement matrix [27-30].

3.1.2.2 For the CLCC50

Fig. 6a shows good adhesion between the matrix and the cork aggregates. In the *Fig. 6b*, we can see that the pores of the cork do not fill with matrix. This phenomenon has already been observed by a number of authors [13, 28]. This is probably due to the phenomenon of water repellency in the water contained in the aggregates, which causes the cleaning of the aggregates pores. The *Fig. 6.c*, relating to CLCC 50 as in the case of the control concrete, reveals the compact aspect of the matrix with the existence of a few pores. We always see a significant presence of dolomite in the samples and we always find the hydration products namely CSH and portlandite. This shows that the introduction of the cork aggregates into the matrix did not modify the structure of the matrix, which has been also confirmed by a number of authors [24, 29- 31]. One can notice the development in the vicinity of the aggregates of needle tuft form generally attributed to CSH.

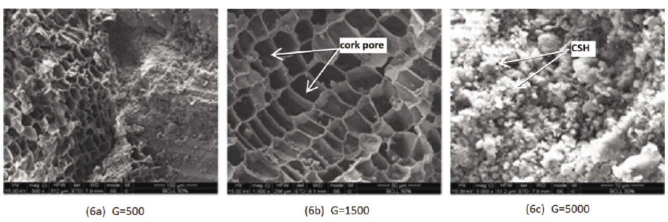

Fig. 6 Micrograph of CLCC50
6. ábra A CLCC50 mikroszkóp alatt

3.2 Chemical compatibility

An infrared spectroscopy analysis was carried out on samples differently dosed in cork aggregates in order to see the influence of the incorporation of cork into the cement matrix. The spectra of the different mixtures are shown in *Fig. 7*. The analysis carried out gives an idea of the effect of cork on the kinetics of formation of hydrated forms of the main components of the material produced. In the area between 1900 cm^{-1} and 711 cm^{-1}, we see some differences in the intensities of certain characteristic bands centered at 1402 cm^{-1}, 1003 cm^{-1} and 871 cm^{-1}. The bands at 1402 cm^{-1} and 871 cm^{-1} are attributed to the vibratory movement of the C-O bonds characterizing the presence of calcium carbonates ($CaCO_3$) [31]. The 1003 cm^{-1} band reflects the vibration of the Si-O bonds, characteristic of the presence of hydrated calcium silicates (C-S-H) [31,32]. In this same area, we see that by adding 70% cork, the intensities of the bands at 1450 and 1003 cm^{-1} decreased. This observation indicates a growth of calcium carbonate when the amount of cork is increased up to 60% in the mixture. Beyond this proportion, there is a decrease in hydrated calcium carbonates and silicates in the medium. This decrease in intensity seems to be due to a modification of the polymerization of C-S-H, but also to carbonates. On the same figure, the band located at 2924 cm^{-1} characteristic of the presence of portlandite does not seem to be affected by the increasing rate of cork in the material. Cork seems to have little effect on the precipitation of portlandite. This indicates that the calcium ions are little affected by the imposed reaction medium. In summary we can say that the incorporation of cork aggregates does not affect hydration except beyond 70% and therefore the cork has good compatibility with cement matrices.

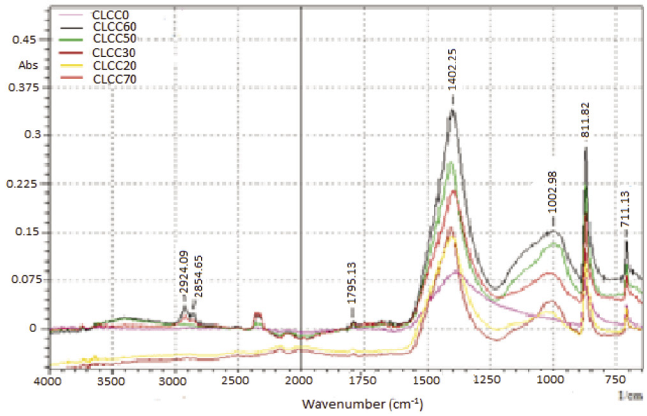

Fig. 7 Infrared spectra of the CLCC
7. ábra A CLCC infravörös spectrum analízisének eredménye

3.3 Mechanical compatibility

3.3.1 Compressive strength

The results concerning the compressive strength tests according to [18]; show a sudden drop in compressive strength when switching from control concrete to concrete dosed at 20%; from 24.4 MPa to 12.22 MPa. The minimum value of the compressive strength is recorded for the maximum dosage of 70%, it is 0.56 MPa with a reduction rate of 97%. The drop in resistance is explained by the substitution of a resistant matrix entity by a less resistant aggregate entity; which has been confirmed by more authors [11, 19, 30, 31]. This property is practically noticed for all lightweight aggregate concretes**.**

3.3.2 Elasticity module

The modulus of elasticity was determined at the age of 28 days during the compression test carried out on cylindrical test tubes ø10×20 cm^3. The modulus value is calculated graphically. It is equal to the slope of the stress-strain curve at 30% of the breaking load. The evolution of the compressive strength as a function of the deformation and according to the dosage of cork aggregates is shown in *Fig. 8*. The test was not carried out on the CLCC 70 sample because of the external morphology of the test tubes. Test specimens which did not allow the location of the gauges. Noticing that the evolution of stress as a function of deformation is similar to that of all concretes. It is characterized by an exponential evolution as a function of the deformation until the breaking. We first find a linear part or elastic phase, then from 30% of the breaking load, the resistance of the composite will evolve slowly and the deformations will be more and more important. Beyond the rupture zone, the deformations will evolve rapidly and a drop in resistance is observed.

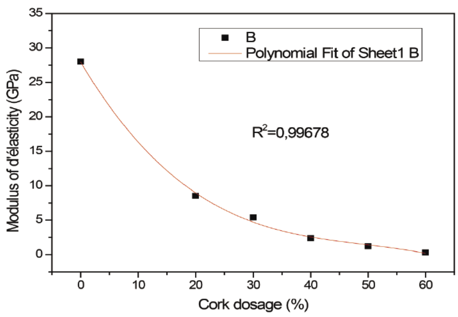

Fig. 8 Evolution of the compressive strength as a function of the deformation of the CLCC
8. ábra A nyomószilárdság alakulása a CLCC deformációjának függvényében

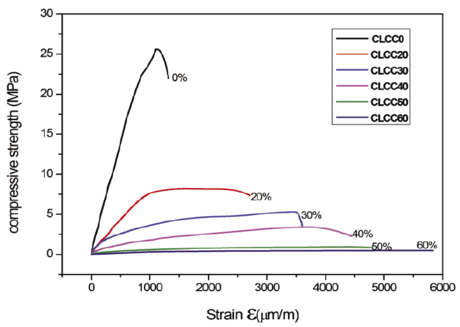

Fig. 9 Evolution of the modulus of elasticity according to the dosage of cork
9. ábra A rugalmassági modulus alakulása a parafa adagolása függvényében

In *Fig. 9* giving the evolution of the modulus of elasticity according to the dosage of cork aggregates, we can clearly see that the value of the modulus decreases as a function of the dosage of aggregates, it goes from a value of 28000 MPa for the reference concrete (CLCC 0) at a value of 8540 MPa for the least lightened concrete (CLCC20) with a reduction rate of 69%. It finally reaches a minimum value of 307 MPa corresponding to the lightest concrete (CLCC 60), i.e. a reduction rate of 98%. By going from control concrete to concrete lightened by cork aggregates, the material becomes less and less rigid; which supports the hypothesis of the replacement of a rigid entity with the same less rigid entity.

4. Conclusions

The aim of this work was to study the compatibility of expanded cork with a cement matrix based on limestone sand. On the basis of a micro-structural analysis we were able to observe a perfect aggregate-matrix bond and that the incorporation of the cork aggregates did not affect the microstructure of the matrix. Infrared spectroscopy analysis allowed us to notice that the incorporation of cork aggregates does not affect the hydration except above 70% and consequently the cork has good compatibility with cement matrices. On the other hand, a mechanical study based on tests of the evolution of the compressive strength as a function of the deformation reveals an elastic incompatibility between the cork and the cement matrix. On the basis of the obtained results and with reference to previous work, we can conclude that expanded cork has better compatibility than the lignocellulosic products generally used.

References

[1] Hernández-Olivares, F., Bollati, M. R., Del Rio, M., & Parga-Landa, B. (1999). Development of cork–gypsum composites for building applications. Construction and Building Materials, 13(4), 179–186. https://doi.org/10.1016/S0950-0618(99)00021-5
[2] Nóvoa, P., Ribeiro, M. C. S., Ferreira, A. J. M., & Marques, A. T. (2004). Mechanical characterization of lightweight polymer mortar modified with cork granulates. Composites science and technology, 64(13-14), 2197-2205. https://doi.org/10.1016/j.compscitech.2004.03.006
[3] Gaye, S., Niang, F., Cissé, I. K., Adj, M., Menguy, G., & Sissoko, G. (2001). Characterisation of thermal and mechanical properties of polymer concrete recycled. J. Sci, 1(1), 53–66.
[4] Chi, J. M., Huang, R., Yang, C.-C., & Chang, J. J. (2003). Effect of aggregate properties on the strength and stiffness of lightweight concrete. Cement and Concrete Composites, 25(2), 197–205. https://doi.org/10.1016/S0958-9465(02)00020-3
[5] Aziz, M. A., Murphy, C. K., & Ramaswamy, S. D. (1979). Lightweight concrete using cork granules. International Journal of Cement Composites and Lightweight Concrete, 1(1), 29–33. https://doi.org/10.1016/0262-5075(79)90006-X
[6] Panesar, D. K., & Shindman, B. (2012). The mechanical, transport and thermal properties of mortar and concrete containing waste cork. Cement and Concrete Composites, 34(9), 982–992. https://doi.org/10.1016/j.cemconcomp.2012.06.003
[7] Mounanga, P., Gbongbon, W., Poullain, P., & Turcry, P. (2008). Proportioning and characterization of lightweight concrete mixtures made with rigid polyurethane foam wastes. Cement and Concrete Composites, 30(9), 806–814. https://doi.org/10.1016/j.cemconcomp.2008.06.007
[8] Fraj, A. B., Kismi, M., & Mounanga, P. (2010). Valorization of coarse rigid polyurethane foam waste in lightweight aggregate concrete. Construction and Building Materials, 24(6), 1069–1077. https://doi.org/10.1016/j.conbuildmat.2009.11.010
[9] Benkreira, H., Khan, A., & Horoshenkov, K. V. (2011). Sustainable acoustic and thermal insulation materials from elastomeric waste residues. Chemical Engineering Science, 66(18), 4157–4171. https://doi.org/10.1016/j.ces.2011.05.047
[10] De-Carvalho, R., Teixeira-Dias, F., & Varum, H. (2013). Cyclic behaviour of a lightweight mortar with cork granulate composite. Composite Structures, 95, 748–755. https://doi.org/10.1016/j.compstruct.2012.08.043
[11] Karade, S. R., & Aggarwal, L. K. (2011). Cement-bonded lignocellulosic composites for building applications. 16th ncb International Seminar on Cement, Concrete and Building Materials At: New Delhi.
[12] Al-Mohamadawi, A., Benhabib, K., Dheilly, R.-M., & Goullieux, A. (2016). Influence of lignocellulosic aggregate coating with paraffin wax on flax shive and cement-shive composite properties. Construction and Building Materials, 102, 94–104. https://doi.org/10.1016/j.conbuildmat.2015.10.190
[13] Nozahic, V., Amziane, S., Torrent, G., Saïdi, K., & De Baynast, H. (2012). Design of green concrete made of plant-derived aggregates and a pumice–lime binder. Cement and Concrete Composites, 34(2), 231–241. https://doi.org/10.1016/j.cemconcomp.2011.09.002
[14] Silva, S. P., Sabino, M. A., Fernandes, E. M., Correlo, V. M., Boesel, L. F., & Reis, R. L. (2013). Cork: Properties, capabilities and applications. International Materials Reviews, 50(6), 345–365. https://doi.org/10.1179/174328005X41168
[15] Şen, A., Marques, A. V., Gominho, J., & Pereira, H. (2012). Study of thermochemical treatments of cork in the 150–400 C range using colour analysis and FTIR spectroscopy. Industrial Crops and Products, 38, 132–138. https://doi.org/10.1016/j.indcrop.2012.01.018
[16] Karade, Sukhdeo R., Irle, M., & Maher, K. (2006). Influence of granule properties and concentration on cork-cement compatibility. Holz Als Roh-Und Werkstoff, 64(4), 281. https://doi.org/10.1007/s00107-006-0103-2
[17] Branco, F. G., Tadeu, A., Belgas, M. D. L., & Reis, C. (2008). Experimental evaluation of the durability of cork concrete. International Journal for Housing Science and Its Applications, 32(2), 149.

[18] Ziregue, A., Khenfer, M. M., Quéneudec-t'Kint, M., & Montrelay, N. (2016). Developmental potentiality of insulating lightweight concrete based on cork and calcareous sand. Journal of Adhesion Science and Technology, 30(9), 934–946.
https://doi.org/10.1080/01694243.2015.1129882

[19] Moreira, A., António, J., & Tadeu, A. (2014). Lightweight screed containing cork granules: Mechanical and hygrothermal characterization. Cement and Concrete Composites, 49, 1–8.
https://doi.org/10.1016/j.cemconcomp.2014.01.012

[20] Magniont, C., & Escadeillas, G. (2017). Chemical composition of bio-aggregates and their interactions with mineral binders. In Bio-aggregates based building materials (pp. 1–37). Springer.

[21] Jami, T., Singh, L. P., & Karade, S. R. (2019.). Vegetal concrete: a foundation for carbon neutral built environment Barnat-Hunek, D., Siddique, R., & \ Lagód, G. (2017). Properties of hydrophobised lightweight mortars with expanded cork. Construction and Building Materials, 155, 15–25.
https://doi.org/10.1016/j.conbuildmat.2017.08.052

[22] Khazma, M., Goullieux, A., Dheillery, R. M., & T'Kint, M. (2008). The use of modified flax shives in cementitious composites and the repercussion of these modifications on their behaviour in the cement matrix. International Conference on Flax and Other Bast Plants.

[23] Pereira, H. (1988). Chemical composition and variability of cork from Quercus suber L. Wood Science and Technology, 22(3), 211–218.
https://doi.org/10.1007/BF00386015

[24] Karade, Sukhdeo R. (2016). Potential of cork cement composite as a thermal insulation material. Key Engineering Materials, 666, 17–29.

[25] Santos, P. T., Pinto, S., Marques, P., Pereira, A. B., & de Sousa, R. A. (2017). Agglomerated cork: A way to tailor its mechanical properties. Composite Structures, 178, 277–287.
https://doi.org/10.1016/j.compstruct.2017.07.035

[26] Tamba, S., Voumbo, L. M., Wereme, A., Gaye, S., & Sissoko, G. (2007). Durabilité des bétons légers à base de copeaux de bois. Journal Des Sciences, 7, 67–72.

[27] Bederina, M., Marmoret, L., Mezreb, K., Khenfer, M. M., Bali, A., & Quéneudec, M. (2007). Effect of the addition of wood shavings on thermal conductivity of sand concretes: Experimental study and modelling. Construction and Building Materials, 21(3), 662–668.
https://doi.org/10.1016/j.conbuildmat.2005.12.008

[28] Barnat-Hunek, D., Siddique, R., & Łagód, G. (2017). Properties of hydrophobised lightweight mortars with expanded cork. Construction and Building Materials, 155, 15-25.
https://doi.org/10.1016/j. conbuildmat .2017.08.052

[29] Barnat-Hunek, D., Widomski, M. K., Szafraniec, M., & Łagód, G. (2018). Impact of different binders on the roughness, adhesion strength, and other properties of mortars with expanded cork. Materials, 11(3), 364.

[30] Belhadj, B., Bederina, M., Montrelay, N., Houessou, J., & Quéneudec, M. (2014). Effect of substitution of wood shavings by barley straws on the physico-mechanical properties of lightweight sand concrete. Construction and Building Materials, 66, 247–258.
https://doi.org/10.1016/j.conbuildmat.2014.05.090.

[31] Fernández-Carrasco, L., Torrens-Martín, D., Morales, L. M., & Martínez-Ramírez, S. (2012). Infrared spectroscopy in the analysis of building and construction materials. Infrared Spectroscopy–Materials Science, Engineering and Technology, 369–382.

[32] Guo, A., Sun, Z., Qi, C., & Sathitsuksanoh, N. (2020). Hydration of Portland Cement Pastes Containing Untreated and Treated Hemp Powders. Journal of Materials in Civil Engineering, 32(6), 04020148.
https://orcid.org/0000-0003-1521-9155

Ref.:
Ziregue, Ahmed – **Krobba**, Benharzallah – **Khenfer**, M. Mouldi – **Dheilly**, Rose-Marie – **Houessou**, Justin – **Quéneudec-t'Kint**, Michèle: *Study of the physicochemical and mechanical compatibility of expanded cork with a cement matrix based on limestone sand*
Építőanyag – Journal of Silicate Based and Composite Materials, Vol. 74, No. 2 (2022), 71–76. p.
https://doi.org/10.14382/epitoanyag-jsbcm.2022.12

GUIDELINE FOR AUTHORS

The manuscript must contain the followings: title; author's name, workplace, e-mail address; abstract, keywords; main text; acknowledgement (optional)**; references; figures, photos with notes; tables with notes; short biography** (information on the scientific works of the authors).

The full manuscript should not be more than 6 pages including figures, photos and tables. Settings of the word document are: 3 cm margin up and down, 2,5 cm margin left and right. Paper size: A4. Letter size 10 pt, type: Times New Roman. Lines: simple, justified.

TITLE, AUTHOR

The title of the article should be short and objective.

Under the title the name of the author(s), workplace, e-mail address.

If the text originally was a presentation or poster at a conference, it should be marked.

ABSTRACT, KEYWORDS

The abstract is a short summary of the manuscript, about a half page size. The author should give keywords to the text, which are the most important elements of the article.

MAIN TEXT

Contains: materials and experimental procedure (or something similar), results and discussion (or something similar), conclusions.

REFERENCES

References are marked with numbers, e.g. [6], and a bibliography is made by the reference's order. References should be provided together with the DOI if available.

Examples:

Journals:

[6] Mohamed, K. R. – El-Rashidy, Z. M. – Salama, A. A.: In vitro properties of nano-hydroxyapatite/chitosan biocomposites. *Ceramics International*. 37(8), December 2011, pp. 3265–3271, http://doi.org/10.1016/j.ceramint.2011.05.121

Books:

[6] Mehta, P. K. – Monteiro, P. J. M.: Concrete. Microstructure, properties, and materials. *McGraw-Hill*, 2006, 659 p.

FIGURES, TABLES

All drawings, diagrams and photos are figures. The **text should contain references to all figures and tables**. This shows the place of the figure in the text. Please send all the figures in attached files, and not as a part of the text. **All figures and tables should have a title**.

Authors are asked to submit color figures by submission. Black and white figures are suggested to be avoided, however, acceptable.

The figures should be: tiff, jpg or eps files, 300 dpi at least, photos are 600 dpi at least.

BIOGRAPHY

Max. 500 character size professional biography of the author(s).

CHECKING

The editing board checks the articles and informs the authors about suggested modifications. Since the author is responsible for the content of the article, the author is not liable to accept them.

CONTACT

Please send the manuscript in electronic format to the following e-mail address: femgomze@uni-miskolc.hu and epitoanyag@szte.org.hu or by post: Scientific Society of the Silicate Industry, Budapest, Bécsi út 122–124., H-1034, HUNGARY

We kindly ask the authors to give their e-mail address and phone number on behalf of the quick conciliation.

Építőanyag – *Journal of Silicate Based and Composite Materials*, Quarterly peer-reviewed periodical of the Hungarian Scientific Society of the Silicate Industry, SZTE. http://epitoanyag.org.hu